

Are Most Low-Luminosity AGN Really Obscured?

Philip F. Hopkins^{1,*}, Ryan Hickox², Eliot Quataert¹, & Lars Hernquist²

¹*Department of Astronomy and Theoretical Astrophysics Center, University of California Berkeley, 601 Campbell Hall, Berkeley, CA 94720*

²*Harvard-Smithsonian Center for Astrophysics, 60 Garden Street, Cambridge, MA 02138*

Submitted to MNRAS, January 18, 2009

ABSTRACT

At low Eddington ratios (\dot{m}), two effects make it more difficult to detect certain AGN given a particular set of selection methods. First, even allowing for fixed accretion physics, at low \dot{m} AGN become less luminous relative to their hosts, diluting their emission; the magnitude of the dilution depends on host properties and, therefore, on luminosity and redshift. Second, low- \dot{m} systems are expected and observed to transition to a radiatively inefficient state, which changes the SED shape and dramatically decreases the luminosity at optical through infrared wavelengths. The effects of dilution are unavoidable, while the precise changes in accretion physics at low \dot{m} are somewhat uncertain, but potentially very important for our understanding of AGN. These effects will have different implications for samples with different selection criteria, and generically lead to differences in the AGN populations recovered in observed samples, even at fixed bolometric luminosity and after correction for obscuration. Although the true Eddington ratio distribution may depend strongly on mass/luminosity, this will be seen only in surveys robust to dilution and radiative inefficiency, such as X-ray or narrow-line samples; by contrast, selection effects imply that AGN in optical samples will have uniformly high Eddington ratios, with little dependence on luminosity, even at low L_{bol} where the median “true” $\dot{m} \lesssim 0.01$. These same selection effects also imply that different selection criteria pick out systems with different hosts: as a result, the clustering of low-luminosity optical/infrared sources will be weaker than that of X-ray sources, and optical/IR Seyferts will reside in more disk-dominated galaxies, while X-ray selected Seyferts will be preferentially in early-type systems. Taken together, these effects can naturally explain long-standing, apparently contradictory claims in the literature regarding AGN Eddington ratio distributions, host populations, and clustering. Finally, we show that if current observed Eddington ratio distributions are correct, a large fraction of low-luminosity AGN currently classified as “obscured” are in fact radiatively diluted and/or radiatively inefficient, not obscured by gas or dust. This is equally true if X-ray hardness is used as a proxy for obscuration, since radiatively inefficient SEDs near $\dot{m} \sim 0.01$ are characteristically X-ray hard. These effects can explain most of the claimed luminosity/redshift dependence in the “obscured” AGN population, with the true obscured fraction as low as $\sim 20\%$.

Key words: galaxies: evolution — cosmology: theory — galaxies: active — quasars: general

1 INTRODUCTION

At the highest luminosities, it is generally accepted that active galactic nuclei (AGN) must lie within a relatively narrow range of black hole masses and Eddington ratios – after all, a quasar with $L_{\text{bol}} \sim 10^{47} \text{ erg s}^{-1}$ requires a $\gtrsim 10^9 M_{\odot}$ black hole (BH); and since this is already on the exponential tail of the black hole mass function, there are vanishingly few $\sim 10^{11} M_{\odot}$ BHs that could give a similar luminosity at low (~ 0.01) Eddington ratios. At low luminosity, however, there is an obvious degeneracy between BH mass and Eddington ratio – a Seyfert ($L_{\text{bol}} \lesssim 3 \times 10^{45} \text{ erg s}^{-1}$) could be

a low-mass BH at high Eddington ratio, or a high-mass BH at low Eddington ratio. Moreover, although there are more low-mass BHs by number density, the duty cycle of low-Eddington ratio activity is higher in many physical models (see e.g. Di Matteo et al. 2003, 2008; Granato et al. 2004; Hopkins et al. 2005d; Lapi et al. 2006; Sijacki et al. 2007), so the two may contribute comparably or in different proportions as a function of luminosity or redshift.

Although it is often implicitly assumed that Seyfert samples selected in the same bolometric (obscuration-corrected) luminosity range are reasonably homogeneous, there are at least two effects – one observational and one physical – that could introduce dramatic differences depending on the wavelengths of identification and the methods used to identify AGN.

* E-mail: phopkins@astro.berkeley.edu

Observationally, even if accretion were self-similar, i.e. there were no change in SED with \dot{m} , many samples implicitly require that the ratio of the AGN optical continuum to host luminosity be above a certain threshold for a galaxy to be identified as an AGN. This criterion varies between different samples and wavelengths, both because of physical differences in the SED shapes of AGN and galaxies, and because of various survey depths and selection methods. Most limited are surveys which select on the basis of “typical” quasar colors dominated by the optical/UV continuum: this implicitly requires that the AGN continuum in the bands of interest be at least comparable to, if not greater than, that of the galaxy.

But even a complete spectroscopic survey looking for Type 1 systems (i.e. the identification of broad lines above some host continuum) implicitly requires an AGN continuum luminosity greater than ~ 0.1 times that of the host (or else the lower-level broad regions of the lines can disappear into the host continuum; see e.g. Vanden Berk et al. 2006; Sánchez et al. 2004; Jahnke et al. 2007). This implicitly sets an Eddington ratio cut as a function of host galaxy properties, where the Eddington ratio \dot{m} (the dimensionless mass accretion rate) is defined as

$$\dot{m} \equiv \frac{\dot{M}}{\dot{M}_{\text{Edd}}} = \frac{\dot{M}}{2.4 M_{\odot} \text{ yr}^{-1} (M_{\text{BH}}/10^8 M_{\odot})} \quad (1)$$

(where the last equality comes from assuming a standard radiative efficiency of $\epsilon_r \sim 0.1$).¹

To assess the effects of dilution quantitatively, assume that a system lies on the Magorrian et al. (1998) relation between BH mass and host bulge stellar mass $M_{\text{BH}} \approx \mu M_{*,\text{bul}}$ (where $\mu \approx 0.001$; Häring & Rix 2004). The total bulge mass is related to the total stellar mass by the bulge-to-total stellar mass ratio $B/T \equiv M_{*,\text{bul}}/M_*$, and the total host galaxy luminosity will be correspondingly given by the stellar mass-to-light ratio in the observed band, $(M_*/L)_{\text{host}}$. The total host luminosity in the observed band is therefore $M_{\text{BH}}/[\mu (M_*/L)_{\text{host}} \times B/T]$. Assuming for simplicity that the radiative efficiency is ~ 0.1 , so that $\lambda = \dot{m}$, the AGN bolometric luminosity is simply $L = \dot{m} L_{\text{Edd}} = \dot{m} (3.3 \times 10^4 L_{\odot}) (M_{\text{BH}}/M_{\odot})$. If the AGN bolometric correction to the observed band is $C_{\lambda} = L_{\text{band}}/L_{\text{bol}}$, then the ratio of the AGN luminosity in the observed band, to the host galaxy luminosity in the same band, will be proportional to the Eddington ratio and given by $\frac{L_{\text{AGN}}}{L_{\text{host}}} \approx 33 \dot{m} C_{\lambda} B/T (M_*/L)_{\text{host}}$ (with $(M_*/L)_{\text{host}}$ in solar units). For the B -band, with typical parameters $C_{\lambda} \approx 1/12$ and $(M_*/L)_{\text{host}} \sim 0.5 - 3 M_{\odot}/L_{\odot}$ (for bolometric corrections, see Richards et al. 2006; Hopkins et al. 2007b), this translates to

$$\frac{L_{\text{AGN}}}{L_{\text{host}}} \approx \frac{\dot{m}}{0.1} \frac{(M_*/L_B)_{\text{host}}}{3 (M_{\odot}/L_{\odot})} \frac{B}{T}. \quad (3)$$

Given typical mass-to-light ratios the AGN will only be visible in color selected samples or identifiable as a Type 1 system by most survey criteria for high accretion rates $\dot{m} \gtrsim 0.01 - 0.1$. Note also the scaling with the host mass-to-light ratio – a younger or more star-forming galaxy is brighter, masking more of the AGN continuum

¹ We also define the dimensionless Eddington-scaled luminosity, λ , in terms of the bolometric luminosity

$$\lambda \equiv \frac{L_{\text{bol}}}{L_{\text{Edd}}} = \frac{L_{\text{bol}}}{1.3 \times 10^{46} \text{ erg s}^{-1} (M_{\text{BH}}/10^8 M_{\odot})}. \quad (2)$$

This is equivalent to \dot{m} when the radiative efficiency is constant, i.e. for \dot{m} above the critical value ~ 0.01 , $\lambda = \dot{m}$. At lower \dot{m} , λ may drop much more rapidly than \dot{m} , if sources become radiatively inefficient (and λ inferred from different bands will be different).

emission, yielding a potential bias against such systems in certain samples of optical/IR-selected AGN (Jahnke et al. 2004, 2006). By contrast, in the X-rays galaxies have much higher M/L – a system with an X-ray luminosity $\sim 10^{43} \text{ erg s}^{-1}$ will be well above the luminosity of even a strongly star-forming host.

Physically, at low Eddington ratio, models predict a transition from a standard, optically thick, UV-bright thin disk to a radiatively inefficient, optically thin accretion flow (see e.g. Narayan & Yi 1994; Esin et al. 1997; Yuan & Narayan 2004; Quataert & Narayan 1999, and references therein), as seen in X-ray binaries (McClintock & Remillard 2006); many observations of both AGN and X-ray binaries support this scenario (Narayan et al. 1996; Meier 2001; Ho 2002; Maccarone et al. 2003; Marchesini et al. 2004; Jester 2005; Cao & Xu 2007).

In radiatively inefficient accretion flows (RIAFs), the thin disk is assumed to evaporate and/or move to much larger radii, and the broad line region and most optical/UV emission declines,² while a hard X-ray spectrum from the thick disk remains. In such a state, the system could still appear in X-ray samples with nearly the same hard X-ray luminosity as it would have if the radiatively efficient solution were extrapolated to the same physical accretion rate, but the system would disappear from optical samples looking for optical/UV light above the host galaxy continuum or for broad-line emission. The systems would likely, however, still appear in *narrow-line* AGN samples, since the central hard X-ray source remains a significant source of photoionization (exactly how the narrow-line properties scale for an incident RIAF spectrum is not certain; a detailed investigation of these scalings will be the subject of future work). Indeed, Kewley et al. (2006) argue that the distinction between Seyferts and LINERs largely owes to Eddington ratio, with LINERs being lower Eddington ratio systems with a harder photoionizing spectrum, consistent with our discussion here.

The models and observations (see references above) indicate that such a transition occurs around an accretion rate $\dot{m} \sim 0.01$. Although the role of such radiatively inefficient states remains controversial, if such a change *does* occur, it would clearly rule out such a mode contributing to the X-ray equivalents of bright quasars. As above, it would require enormous BHs to produce such a luminosity at such low Eddington ratio – but RIAFs could easily contribute significantly to lower-luminosity samples. A $\sim 10^8 M_{\odot}$ BH is still radiating at nearly $10^{43} \text{ erg s}^{-1}$ in hard X-rays at $\dot{m} = 0.01$, and the total number density of such systems is $\sim 10^{-2} \text{ Mpc}^{-3}$. Only $\sim 1 - 5\%$ of them need to be active at these low Eddington ratios to account for the entire observed population of such X-ray sources in the local universe (Ueda et al. 2003). But with rapidly declining optical luminosity and disappearing broad line regions, such sources may vanish from most Type 1 optical samples.

Together, these effects could lead to very different Seyfert populations being observed in different bands or with different selection criteria. They also relate to a physical distinction in how AGN may be fueled. A low-mass BH at high Eddington ratio is likely to be in a gas-rich, disk dominated system (given the typical

² Note that, in realistic models, the broad line region does not simply vanish instantly, but rather moves outwards with the thin disk and so declines with the optical/IR luminosity of the AGN. Of course, this decline, relative to the host, will still yield a system that will not appear in traditional broad-line samples. Observationally, the presence of some weak broad lines, even in very low accretion rate systems (many of which show continuum or polarization evidence of being in a RIAF/thick disk state inwards of the thin disk) has been noted down to accretion rates $\dot{m} \sim 0.001$ (see e.g. Ho 1999; Moran et al. 2000; Tran 2003; Hao et al. 2005b,a).

properties of the expected low bulge-mass host). Fueling growth at these luminosities and masses need not be related to violent events such as major mergers of galaxies, but may be achievable by common mechanisms such as the stochastic accretion of molecular clouds (Hopkins & Hernquist 2006), gas inflow in barred systems (Jogee 2006), and minor mergers (Younger et al. 2008). Although the fueling mechanisms can be relatively mundane, the small-scale physics present are – being systems at high Eddington ratio – simply a scaled-down version of quasar activity, and as such represent a continuation of a feedback-regulated scenario, where high-Eddington ratio activity (implying rapid BH growth) is truncated by AGN feedback at a critical mass/luminosity corresponding to the observed M_{BH} -host spheroid correlations (Di Matteo et al. 2005), and the AGN rapidly decays to lower luminosities with some characteristic power law-like light curve decline (Hopkins & Hernquist 2006, 2009).

On the other hand, a high-mass BH at a low Eddington ratio, living in a massive host, is a natural consequence of a system already in its late-time decay phase, having previously gone through a state of rapid accretion, feedback, and self-regulated growth. It is possible, of course, to re-ignite such a system by the accretion of new cold gas in a minor merger or via secular instabilities, but this will more likely lead to a brief new burst of bright quasar activity before declining again to a long-lived low Eddington ratio mode. Simulations and observations suggest that systems can linger in this “decaying” mode for \sim Gyr to a Hubble time (Yu et al. 2005; Volonteri et al. 2006; Hopkins et al. 2005b,c, 2008b; Yu & Lu 2008; Ciotti et al. 2009), either in such a post-merger steadily declining level of activity or eventually in an equilibrium, accreting e.g. hot gas from the diffuse, pressure supported gaseous halo in the spheroid or from stellar winds (the distinction between this “steady state” accretion and a “smooth decline” from initial high levels of activity triggered in e.g. mergers is largely semantic – the two likely blend seamlessly into one another).

Given the potential importance of these observational selection effects, and the theoretical interest in understanding different modes of accretion and their implications for observed AGN samples, it is of considerable interest to develop predictions and observational discriminants between these modes of accretion; it is also important to recognize the observational selection effects that might lead to the preferential selection of different populations. Any observations intending to study AGN host galaxies, fueling mechanisms, and evolution must account for such distinctions. In this paper, we adopt a simple and general model for AGN lightcurves and use it to illustrate the effects of dilution and radiative efficiency on observational inferences of the Eddington ratio distributions, obscured fractions, clustering, and host galaxy morphologies of AGN as a function of luminosity and redshift. Recognizing these biases, however, the same observations, coupled with models such as those presented here, can be used to break degeneracies between e.g. populations with different BH masses and Eddington ratios at fixed luminosity; these can ultimately be used to constrain models for the long-term evolution of AGN across many different stages of galaxy evolution.

In § 2 we outline a simple semi-empirical way of estimating the “intrinsic” BH mass/Eddington ratio distribution at a given AGN luminosity; we further demonstrate how dilution and radiative inefficiency can change this distribution. We also compare to observations in different wavebands and discuss how the observational inferences relate to theoretical models (taking into account selection effects). In § 3 we examine how dilution and radiative inefficiency influence estimates of the “obscured” or Type 2 AGN

fraction. In § 4 we investigate how the observed clustering of AGN as a function of wavelength, luminosity, and redshift can depend on the sample selection criteria, and in § 5 we examine how these effects can change the resulting host morphology distributions at a given AGN luminosity. Finally, in § 6 we summarize our results and outline observational tests that can resolve the degeneracies highlighted in this paper.

For ease of comparison, we convert all observations to bolometric luminosities given the appropriate bolometric corrections from Hopkins et al. (2007b) (see also Richards et al. 2006), based on the observations in Elvis et al. (1994); George et al. (1998); Vanden Berk et al. (2001); Perola et al. (2002); Telfer et al. (2002); Ueda et al. (2003); Vignali et al. (2003). We adopt a $\Omega_{\text{M}} = 0.3$, $\Omega_{\Lambda} = 0.7$, $H_0 = 70 \text{ km s}^{-1} \text{ Mpc}^{-1}$ cosmology and a Salpeter (1955) stellar initial mass function (IMF), and normalize all observations and models appropriately (note that this generally affects only the exact normalization of quantities here, not the qualitative conclusions). All magnitudes are in the Vega system.

2 EDDINGTON RATIO DISTRIBUTIONS AND AGN SELECTION

In order to construct plausible estimates for the effects of dilution, we begin with a model for the AGN Eddington ratio distribution. We follow the methodology of Hopkins et al. (2006a): given the observed AGN luminosity function, a model for the average AGN lightcurve (or lifetime) uniquely translates to an Eddington ratio distribution as a function of luminosity and redshift. For example, if lightcurves were step-functions with some “on” and “off” m , the Eddington ratio distribution would simply be the corresponding δ -functions. Here, we adopt a simple parameterization of the lifetime/lightcurve motivated by hydrodynamic simulations with BH feedback (Hopkins et al. 2005a, 2006b). The lightcurves, Eddington ratio distributions, and detailed comparison of both with observations are presented in Hopkins & Hernquist (2009); a number of other details and observational tests of the model (comparison with e.g. host mass distributions, clustering, and other properties) are presented in a series of papers (e.g. Hopkins et al. 2005b, 2006a, 2008b). We refer the interested reader to these works for more details, but briefly summarize the methodology here.

We begin with the observed (redshift-dependent) bolometric quasar luminosity function, here from the compilation of observations in (Hopkins et al. 2007b) (see also Shankar et al. 2009, and references therein). We parameterize the AGN lifetime (the statistical representation of the lightcurve; namely, the differential time spent per unit luminosity, for a BH of a given mass) with a simple Schechter-function fit: $dt/d\log L \approx t_0 (L/L_0)^{-\alpha} \exp(-L/L_0)$. The normalization $t_0 \sim 10^8 \text{ yr}$ is the lifetime of high-Eddington ratio activity and is comparable to the Salpeter time (Salpeter 1964) for the e -folding of a BH at the Eddington limit; this estimate is also reasonably consistent with observations (e.g., Martini 2004 and references therein). The “cutoff” at $L_0 \approx 0.4 L_{\text{Edd}}$ is the expected cutoff near the Eddington rate for the given BH mass, and $\alpha(M_{\text{BH}}) \sim 0.5$ is a weak mass-dependent scaling (see Hopkins & Hernquist 2009).

The formalism used here can represent a range of realistic AGN light curve shapes, including those with an exponential rise/fall, those with a range of variability power spectra, and those with a late-time power-law like decay as predicted in a variety of self-regulated growth scenarios (Menci et al. 2003; Granato et al. 2004; Sazonov et al. 2004; Hopkins & Hernquist 2006; Ciotti & Ostriker 2007). Adjusting the model parameters to

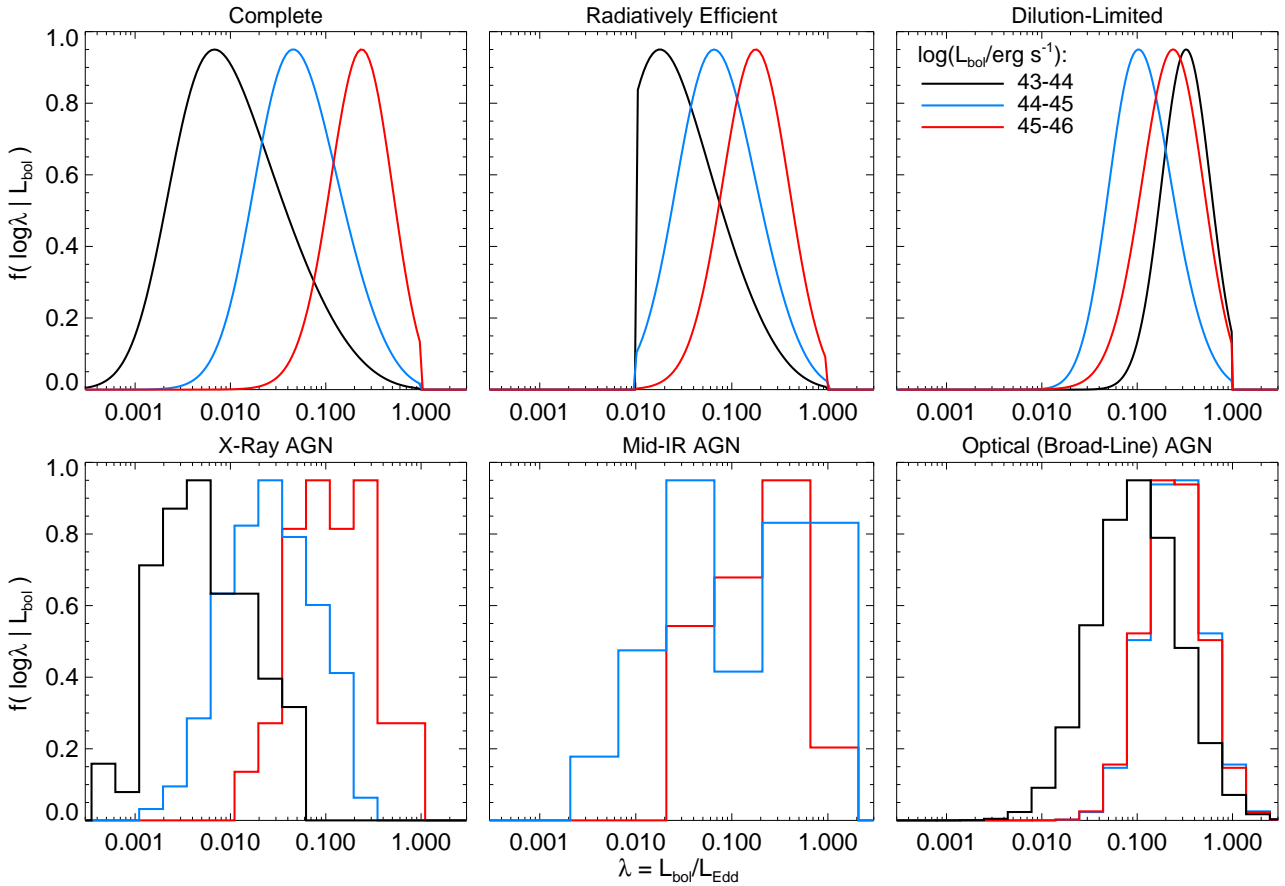


Figure 1. *Top:* Distribution of Eddington ratios (normalized $dN/d\log\lambda$, where $\lambda \equiv L_{\text{bol}}/L_{\text{Edd}}$) at a given AGN bolometric luminosity (as labeled), at $z \sim 0-1$, derived from the models described in §2. *Left:* “True” distribution – i.e. that in a “complete” sample that can recover all AGN regardless of radiative efficiency and/or dilution (appropriate for deep X-ray and host-galaxy selected deep narrow-line surveys). *Middle:* Distribution if only “radiatively efficient” AGN are detected, where we assume that thin disks disappear below $\dot{m} = 0.01$. This is appropriate for surveys relying on broad lines and/or optical/IR continuum features (however deep). *Right:* Distribution if only AGN with optical/IR luminosities greater than $\sim 10\%$ of the host galaxy in the same band are selected. This is required for any color/continuum selection in these wavelengths, but also applies to most searches for broad-line signatures in complete galaxy samples (especially if the width of those lines is desired). Note the increasingly narrow range in the observed Eddington ratio distribution – and decreasing dependence on L – as these selection effects are included. This is because low- λ AGN are potentially radiatively inefficient, and relatively less luminous relative to their hosts. *Bottom:* The observed Eddington ratio distributions for observed samples of AGN at a given AGN bolometric luminosity (based on bolometric correction from the X-ray or IR luminosities). *Left:* X-Ray selected AGN from the observations in Hickox et al. (2009), where the effects of radiative efficiency and dilution are weak. This agrees well with the prediction for a “complete” sample at each L_{bol} . *Center:* Mid-IR selected AGN, where radiatively inefficient AGN will be under-luminous (and dilution effects enter as well, albeit to a lesser extent), also from Hickox et al. (2009). The distribution is less luminosity-dependent, in reasonable agreement with predictions for such a sample. *Right:* Optically selected broad-line AGN from Kollmeier et al. (2006, at $L_{\text{bol}} > 10^{44} \text{ erg s}^{-1}$) and Greene & Ho (2007, at $L_{\text{bol}} < 10^{44} \text{ erg s}^{-1}$); for these samples radiatively inefficient AGN will not appear and AGN with luminosities much less than their hosts will also be excluded. Here there is almost no dependence of Eddington ratio on luminosity, with all sources having high $L_{\text{bol}}/L_{\text{Edd}} \sim 0.1-1$, as predicted for samples with similar observational selection criteria.

cover this broad range of possibilities, we find that our qualitative conclusions are relatively robust. Given this, we use the values quoted above based on hydrodynamic simulations. Likewise, varying the choice of the bolometric QLF adopted by using just a subset of the observations compiled in Hopkins et al. (2007b) makes little difference.

Together, the bolometric luminosity function and prescription for AGN lifetimes specify the Eddington ratio distribution: the number at a given luminosity is known, and since the probability of a given system being at a given luminosity is trivially related to the shape of the lightcurve, one can de-convolve to determine the underlying BH mass/Eddington ratio distribution. Once this is specified, the most important aspect of the model is specified. Given the observed $M_{\text{BH}} - M_{\text{bulge}}$ relation (with normalization and scatter taken from Häring & Rix 2004), we can convert

this to a host bulge mass distribution. Likewise, given the observed correlation between galaxy mass and bulge-to-total mass ratio (B/T), and its scatter (here from Balcells et al. 2007), we can convert this to a distribution in total host galaxy mass and/or host morphology. Given some template galaxy SED or, more simply, an average stellar mass-to-light ratio as a function of galaxy mass (and redshift), well-determined in a number of studies (see e.g. Bell et al. 2003; Conroy & Wechsler 2009; Ilbert et al. 2009; van Dokkum et al. 2004; Kassin et al. 2007; Moster et al. 2009), we trivially convert the host mass to a host luminosity distribution. Note that directly using the observed correlation between BH mass and total host luminosity (e.g. Kormendy & Richstone 1995) – accounting for its larger scatter – yields a nearly identical result.

In Hopkins & Hernquist (2009), we compare the distributions of BH and host properties inferred via the above procedure with

the distribution of Eddington ratios and BH and host masses measured in deep narrow line samples at $z = 0$ and inferred at $z = 1$ (from Heckman et al. 2004; Hopkins et al. 2006c; Yu et al. 2005; Merloni & Heinz 2008). The agreement is good over the observed range from $M_{\text{BH}} \sim 10^6 - 10^9 M_{\odot}$. Likewise, comparing with the host galaxy mass, luminosity, and color distributions in these low-redshift samples (Kauffmann & Heckman 2008) and smaller high-redshift samples (e.g. Peng et al. 2006) yields reasonable agreement. So these simple analytic models at least provide a good approximation to the actual observed distributions in the local Universe.

Given the above models, we take into account the effects of dilution and/or radiatively inefficient accretion by considering three simplified models for how the “true” distribution might be observed:

- (1) Complete: All sources at the given bolometric luminosity are included, regardless of Eddington ratio or host properties. This might be representative of e.g. deep X-ray surveys (modulo Compton-thick sources) or narrow-line optical surveys.

- (2) Brighter than Host/Dilution-Limited: Given the observed dependence of galaxy mass-to-light ratios on stellar mass in various bands (Bell et al. 2003), we convert our host bulge plus disk mass distribution to a host luminosity distribution as noted above, and compare it to the observed AGN luminosity in the same band (with bolometric corrections from Hopkins et al. 2007b). We include objects only above some threshold in the observed band; specifically, those sources for which the B -band luminosity of the AGN is larger than 10% of its host luminosity in the same band. This is appropriate for AGN samples selected on the basis of their broad-band IR-UV colors.

- (3) Radiatively Efficient only: We include sources with Eddington ratios above some critical threshold, $\dot{m} > \dot{m}_{\text{crit}}$, where we take $\dot{m}_{\text{crit}} = 0.01$ (see § 1). If there is indeed a change in accretion physics around this accretion rate, then such a cutoff is appropriate for samples that select AGN based on broad-band luminosities or colors in the UV, optical, or near infrared, or surveys that depend on identifying Type 1 signatures such as the presence of broad emission lines.

Figure 1 shows the inferred distribution of Eddington ratios at various bolometric luminosities for the three different sample cuts above.³ At a given luminosity (unlike at a given BH mass), the Eddington ratio distribution is roughly a lognormal distribution, albeit with some non-negligible skewness (as inferred by e.g. Fine et al. 2008). This is because, at sufficiently low \dot{m} , arbitrarily high- M_{BH} BHs would be implied (at fixed L), but the number of such systems is vanishingly small. Figure 1 shows that the Eddington ratio distribution can be dramatically affected by different observational limits, becoming much narrower and more weakly dependent on luminosity when luminosity/Eddington ratio cuts are applied.

Figure 2 shows the median and 1σ dispersions in Eddington ratio as a function of luminosity at $z = 0.5$, based on approximating

³ In order to be consistent with typical observational procedures, the “bolometric luminosity” plotted here is technically the bolometric luminosity that would be inferred based on the actual luminosity in some band (given the bolometric corrections from Hopkins et al. 2007b, used throughout). If there is no qualitative change in SED shape with \dot{m} , this is the true bolometric luminosity, but in the “radiatively efficient” sample cut above, this represents instead the inferred luminosity assuming, as is typically done, a standard high \dot{m} SED, even if the system is in fact radiatively inefficient and thus possesses an intrinsically different SED.

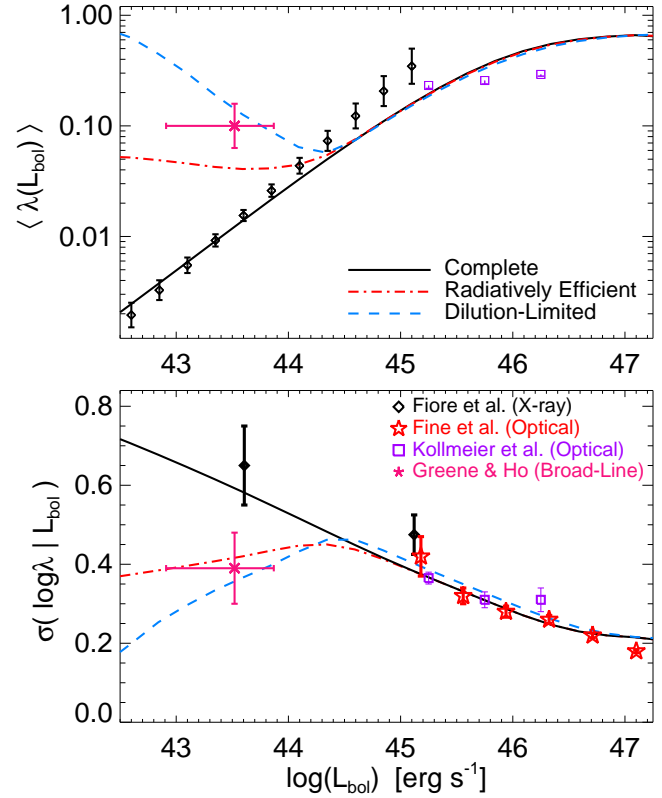


Figure 2. Median Eddington ratio λ and 1σ dispersion in Eddington ratio at a given bolometric AGN luminosity (as in Figure 1). We compare the predictions for the various selection criteria in Figure 1 with the observed distributions inferred from the distribution of X-ray to host luminosities in optically obscured AGN (Fiore et al. 2003; Hasinger 2008; Hickox et al. 2009, black diamonds) (translating host luminosity to average BH mass), and from the distribution fitted to broad-line optical samples in Fine et al. (2008) from the 2dF, Kollmeier et al. (2006) from AGES, and Greene & Ho (2007) using the optical virial (line-width) BH mass estimators. At high- L , all the selection criteria yield similar results in good agreement with the observations – almost all systems at these L are radiatively efficient and bright relative to their hosts. At low- L , the X-ray and broad-line results disagree – the low mean λ and wide dispersion in λ near $L \sim 10^{43.5} - 10^{44} \text{ erg s}^{-1}$ ($L_{2-10\text{keV}} \sim 0.3 - 1 \times 10^{43} \text{ erg s}^{-1}$) for the X-ray sample is consistent with the predictions for a complete sample, while the large $\lambda \sim 0.1$ and small dispersion in the broad-line sample of Greene & Ho (2007) agrees with the predictions for a restricted (dilution or efficiency-limited) sample.

the predicted distributions as lognormal (we use the IPV width to prevent bias from outliers or skewness). We compare the predictions with several observational estimates.

Fine et al. (2008) consider the Type 1 quasar population near $z \approx 1$ in the 2dF survey, and estimate the distribution of BH masses in narrow bins of luminosity relying on the commonly adopted virial BH mass estimators (see e.g. Vestergaard & Peterson 2006, and references therein). This allows them to consider the distribution of BH masses via this proxy as a function of luminosity down to near Seyfert luminosities. Because the width of the distribution can be determined without relying on the (systematically still uncertain) absolute normalizations of these calibrators, the authors decline to estimate absolute Eddington ratios (although a rough estimate suggests they lie between $\sim 0.1 - 1$, as predicted here). Kollmeier et al. (2006) use the same technique over a narrow luminosity range of Type 1 AGN in the AGES survey. At yet

lower-luminosities, Greene & Ho (2007) study a sample of local broad-line AGN from the SDSS down to extremely low luminosities $L_{\text{bol}} \sim 10^{43} \text{ erg s}^{-1}$ ($L_{\text{H}\alpha} \sim 10^6 L_{\odot}$).

X-ray observations can study Type 2 objects at comparably low luminosities, where the optical light is dominated by the host galaxy and therefore a host galaxy stellar mass (and corresponding BH mass, adopting the observed $M_{\text{BH}} - M_*$ relation from Marconi & Hunt 2003) can be estimated. It is well-established that in this regime the optical luminosity of the galaxy is approximately constant while the X-ray luminosity changes, implying that at lower- L the X-ray luminosity function becomes largely a sequence in Eddington ratio (Fiore et al. 2003; Barger et al. 2005; La Franca et al. 2005; Silverman et al. 2005b,a, 2008b; Hasinger 2008; Hickox et al. 2009).

Figure 2 shows the results of the X-ray sample of Fiore et al. (2003), where the optical R -band luminosity is converted to a stellar mass based on the age and mass-dependent observed mean M/L ratios in Bell & de Jong (2000) and Bell et al. (2003). We have recalculated these comparisons using the samples of Hasinger (2008) and Hickox et al. (2009) and obtain the same result; changing the assumed host M/L within uncertainties makes little difference.

Figure 2 shows that the faint X-ray results agree with optical results at high luminosities (as do the models). At low luminosities, however, the X-ray results find that the median accretion rate decreases and the scatter increases, in agreement with our predictions for a “complete” sample.⁴ Narrow-line AGN samples also find a similar trend to that predicted for the “complete” sample. Hao et al. (2005a,b) find that host galaxy luminosity remains \sim constant as AGN luminosity declines, down to very low luminosities $L_{\text{bol}} \sim 10^{42} \text{ erg s}^{-1}$. Kauffmann et al. (2003) make this explicit, with Eddington ratios distributions moving to lower $\dot{m} \lesssim 0.01$ and spanning an ~ 1 dex range at the lowest luminosities.

However, the Greene & Ho (2007) optical results are quite different: they find a median Eddington ratio $\dot{m} \sim 0.1$ with a relatively small (factor ~ 2) scatter, similar to what is found in the optical broad-line samples at three orders of magnitude higher luminosity. At the same bolometric luminosity, the median \dot{m} is much higher than that in X-ray selected samples and the spread is smaller. This result agrees well with the expectation from our selection effect-limited models: because only sources with clear optical broad-line signatures of a “quasar” are selected, low-Eddington ratio systems which are simply underluminous relative to their hosts (and may also be radiatively inefficient) are excluded.

Figure 1 directly compares the Eddington ratio distributions observed in different wavebands and the model predictions, for AGN spanning three orders of magnitude in bolometric luminosity. In the X-ray sample of Hickox et al. (2009), the observed distributions agree well with the expectation from the “complete” model – in particular, the median Eddington ratio clearly shifts to lower values with decreasing luminosity in the manner predicted. On the other hand, in infrared or optically-selected samples, the results are similar to that seen in Figure 2: observed Eddington ratio distributions are much narrower and less luminosity-dependent.⁵ This

⁴ We expect this to be independent of whether or not Compton-thick sources are missed in hard X-ray samples, since we are here assuming that whatever “true” obscuration is present is not host-property dependent. This may be uncertain, but if it were not so, it would only strengthen our conclusions.

⁵ The observed infrared distributions are somewhat broader than the predictions; most of this can be attributed to scatter in the bolometric corrections and BH mass estimators. The predicted distributions would also be

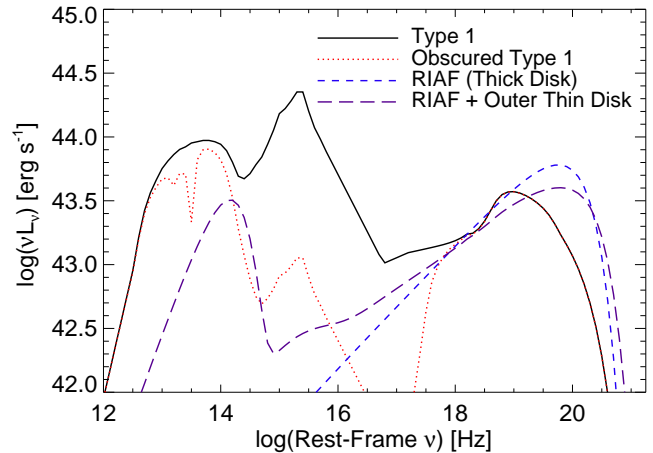


Figure 3. AGN SEDs: an unobscured, Type 1 QSO (from Hopkins et al. 2007b), and that spectrum obscured by a column with $N_H = 10^{22} \text{ cm}^{-2}$ (with Milky Way gas-to-dust ratios and an SMC-like reddening curve from Pei 1992, and a small $\sim 5\%$ optical/UV scattering component); we also show the predicted spectrum of an optically thin RIAF (Quataert & Narayan 1999) and a model with an inner RIAF and outer (truncated) thin α -disk. Without detailed SEDs, the RIAF models are indistinguishable from obscuration in the optical, and yield power-law like X-ray spectra with hardnesses similar to obscured Type 1 objects. The luminosities are arbitrarily scaled to be comparable to the systems of interest in X-rays.

is more pronounced for the optical sample than the infrared one, but this too could be anticipated. In the optical, dilution is more severe than in the infrared; however, radiative efficiency, if important, should influence the results in both these bands similarly.

3 IMPLICATIONS FOR “OBSCURED” AND TYPE 2 POPULATIONS

Given the significant differences in the Eddington ratios selected in different samples, we now study whether this will affect other inferences drawn from AGN samples. We first focus on the implications for “obscured” and “unobscured” populations. Ideally, AGN would be observationally classified as obscured on the basis of detailed multiwavelength SED estimates – in particular X-ray spectroscopy, which can definitively show an absorption cutoff (although even in this case, Compton-thick sources will not be identified), and corresponding absorption spectra in the infrared. Although there are well-observed systems where the presence or absence of actual dust/gas obscuration can be unquestionably established (e.g. Weymann et al. 1981; Laor et al. 1997; Zakamska et al. 2004), these observations are prohibitively time-consuming for the high redshift surveys that are used to try to statistically quantify obscured fractions as a function of e.g. luminosity and redshift. As a consequence, AGN in these samples are typically classified as “obscured” on the basis of simplified proxies: the absence of dominant AGN luminosity/colors (or a broad-line SED) in the optical, or X-ray hardness. If however, the AGN emission is not dominant in the optical, these might masquerade as “obscured” sources in observed samples.

Figure 3 illustrates these issues. We first compare template

broader if the transition to radiative inefficiency were more gradual than we model.

SEDs of a Type 1 quasar and a “true” obscured quasar. The obscured system is the product of the Type 1 template attenuated by a column of $N_H = 10^{22} \text{ cm}^{-2}$, with a Milky Way-like gas-to-dust ratio, solar metallicity, SMC-like dust reddening curves fitted in Pei (1992), and photoelectric absorption in the X-ray following Morrison & McCammon (1983); for details see Hopkins et al. (2006a). Differences in e.g. the gas-to-dust ratios and reddening curves of AGN will somewhat alter the quantitative details here, but our qualitative conclusions below are not sensitive to these choices.

Dilution can easily hide an AGN in the optical or infrared; recall (eq. 3) that at an Eddington ratio $\dot{m} \sim 0.01$, even if the system is still radiatively efficient, the *B*-band luminosity of the AGN is $< 10\%$ of the host galaxy luminosity in a relatively old elliptical host galaxy (with high M_*/L and B/T); in a young spiral galaxy (with typical $B/T \lesssim 0.2$; Weinzirl et al. 2009) that might host a $\sim 10^6 - 10^7 M_\odot$ BH, the fraction of the optical light drops to $< 1\%$. At these ratios, the galaxy continuum dominates, and the system would be classified as Type 2 or obscured according to any color, continuum, or broad-band based photometric criteria. The “true” AGN SED is unobscured, but the optical/IR light is predominantly galaxy light (by definition, in this regime). Broad lines would in principle be detectable, but only with very deep observations – the peak broad line height in the optical SED, given the composite quasar SED (see Vanden Berk et al. 2001), would appear as a $< 2\%$ correction to the continuum for the star-forming case above (comparing to model SEDs from Bruzual & Charlot 2003). This is prohibitively time-consuming for all but a few local, well-studied systems (even in the early type galaxy, reliable identification of a single broad line would require $S/N \sim 30$ spectroscopy; typical SDSS spectra, for comparison, are $S/N \sim 6$, leading to difficulty making broad-line identifications when the AGN fraction falls below $\sim 30 - 50\%$; Vanden Berk et al. 2006). In practice, most objects in the large samples used to classify systems as obscured or unobscured require that the AGN continuum dominate in the optical in order to define a system as Type 1 (in detail, systems are often classified as Type 1 or 2 on the basis of whether a single galaxy or AGN template provides a better fit to the optical; in such a case, the requirement that the AGN dominate the light is explicit).

Figure 3 further compares the Type 1 and true obscured SEDs with two template spectra for radiatively inefficient accretion models. First, we consider a RIAF around a $5 \times 10^8 M_\odot$ BH with a dimensionless accretion rate of $\dot{m} = 0.01$. The dimensionless spectrum $\nu L_\nu / L_{\text{Edd}}$ is a weak function of black hole mass at fixed \dot{m} , and so can be trivially scaled to different luminosities (in Figure 3 we arbitrarily scale the SEDs to be comparable in X-ray luminosity, since we will be considering samples observed in fixed luminosity bins). The spectral calculations here are based on the models of Quataert & Narayan (1999), to which we refer the reader for details. The one important difference is that we use the results of Sharma et al. (2007) for electron heating in RIAFs. One uncertainty in the modeling is that RIAFs have strong outflows that may carry away a significant fraction of the mass supplied at large radii (Blandford & Begelman 1999); for the models of interest here, the emission is largely produced at small radii close to the black hole horizon, and so the spectrum is not strongly sensitive to the presence of outflows so long as the accretion rates quoted here are interpreted as \dot{m} at small radii close to the black hole’s horizon; equivalently, we can consider systems at fixed luminosity regardless of the large-scale accretion rates producing that luminosity. In short, this affects only the ratio of the mass accretion rate to luminosity; since we will consider objects at fixed luminosity, this makes no difference.

At the accretion rates relevant to this paper, theoretical models and observations of both X-ray binaries (e.g. Esin et al. 1997) and AGN (e.g. Quataert et al. 1999) suggest that the inner RIAF is likely surrounded by an outer thin disk. The latter produces a non-negligible optical-IR flux, although much less than a standard radiatively efficient disk would produce if it extended close to the black hole. In addition, the disk photons inverse Compton cool the inner RIAF, softening the X-ray spectrum. This is shown explicitly in Figure 3 where we also plot the spectrum for a model in which the transition from thin disk (modeled as a standard Shakura & Sunyaev 1973, α -disk) to RIAF occurs at 100 Schwarzschild radii.

In either case, it is straightforward to see how the RIAF spectra would be observationally equivalent to an obscured AGN in the optical. Interestingly (as we discuss further below), the RIAF spectra are also hard power-laws in the X-rays: their hardness can be similar to a gas-obscured intrinsic Type 1 AGN spectrum.

Given our models for the Eddington ratio distributions of AGN, we can estimate the fraction of systems that would erroneously be classified as optically “obscured” because of either dilution or, more speculatively, a transition to radiatively inefficient accretion. This is simply the fraction, relative to a “complete” sample, that meet our previous criteria (2) or (3), respectively. Figure 4 shows the resulting “obscured” fraction as a function of luminosity and Figure 5 shows the “obscured” fraction as a function of redshift. Because at lower luminosities the fraction of low-Eddington ratio systems is larger (see § 1), this generically leads to a decreasing “obscured” fraction with increasing luminosity. Moreover, because the shape and break location of the luminosity function evolve with redshift (implying that the distribution of Eddington ratios shifts accordingly in high-mass BHs; recall here we adopt the QLF evolution from the compilation in Hopkins et al. 2007b, but other observations yield similar results), at fixed luminosity there can be a weaker but still non-zero dependence of the “obscured” fraction on redshift (Fig. 5). Specifically, it is well-established that more massive BHs are preferentially active at higher redshifts; as such, it is possible that a population at fixed (sub- L_*) luminosity includes a larger fraction of high-mass BHs at low Eddington ratio, leading to larger (fractional) dilution. In addition, for the same host galaxy mass, star formation rates (and therefore stellar population luminosities) increase with redshift.

The trends we find are similar to the increasingly well-established observed trends in various samples (Hill et al. 1996; Simpson et al. 1999; Willott et al. 2000; Simpson & Rawlings 2000; Steffen et al. 2003; Ueda et al. 2003; Grimes et al. 2004; Hasinger 2004; Sazonov & Revnivtsev 2004; Barger & Cowie 2005; Simpson 2005; Hao et al. 2005b; Gilli et al. 2007; Hickox et al. 2007; Hasinger 2008). We compare the observations from Hasinger (2008), a hard X-ray selected sample, to our simple estimates in Figures 4 & 5. Although some of the observationally identified “obscured” systems are almost certainly obscured in the real, traditional sense (especially at the highest luminosities), our estimates suggest that a reasonable fraction of the very high inferred obscured fractions (approaching unity) may owe to these selection effects, rather than to actual dust/gas obscuration.

In detail, even with the strong assumptions in Figures 4 & 5, that all objects below $L_{B, \text{AGN}}/L_{B, \text{host}} < 0.1$ (dilution-limited) or below $\dot{m} = 0.01$ (radiative efficiency-limited) are classified as “obscured,” we do not reproduce the full observationally inferred obscured fraction. Including a constant (luminosity and redshift-independent) “true” obscured fraction of 0.2, our inferred “ob-

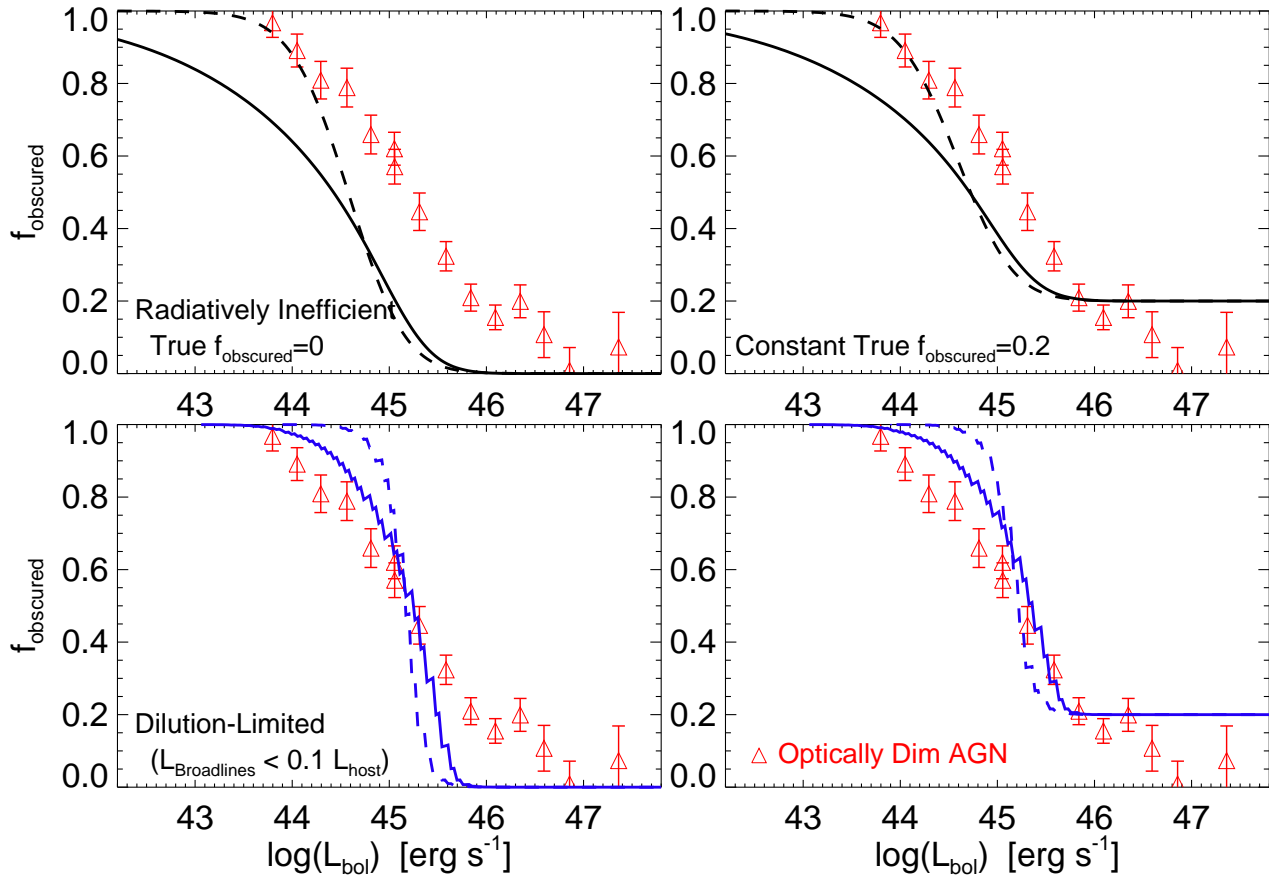


Figure 4. Predicted fraction of AGN at a given bolometric luminosity that would be classified as “obscured” in optical samples. *Top Left:* Fraction of objects at a given bolometric luminosity that are radiatively inefficient and thus would be absent in optical samples. Solid and dashed lines correspond to the allowed range of Eddington ratio distributions derived from models and observations (see Hopkins & Hernquist 2009). We compare with the observed “obscured” fraction from the observations in Hasinger (2008), where (X-ray selected) objects are labeled “obscured” based on the lack of dominant broad-line AGN in the optical. *Top Right:* Same prediction, but with a constant (luminosity-independent) fraction = 0.2 of genuinely obscured sources added at all L . The combination of a true 20% obscured fraction and radiatively inefficient accretion at low L can approximately reproduce the observationally inferred “obscured” sources. *Bottom Left:* As top left, but showing the predicted fraction of systems which will drop out in the optical from a dilution-limited sample (or samples where Type 1/2 classification is based on optical/UV/IR colors, continuum, presence of broad-lines, or goodness-of-fit of template AGN versus galaxy SEDs in the optical/IR). *Bottom Right:* As bottom left, with a constant fraction = 0.2 of genuine obscured sources. The observed trend of “obscured” fractions with luminosity can be explained primarily by these Eddington ratio effects, with a true obscured fraction ~ 0.2 that is much less dependent on luminosity than a direct interpretation of the data would imply.

scured” population is similar to observational estimates as a function of both luminosity and redshift (right-hand panels in Figs. 4 & 5). Thus, although some genuine obscuration is required, it might be as low as $\sim 20\%$ of the population, significantly less than what is typically inferred in low-luminosity AGN samples; more important, the majority of the inferred luminosity and redshift dependence in observed samples can be accounted for by the effects of a non-trivial Eddington ratio distribution and the inevitable selection effects in optical continuum or broad-line samples.

Note that we are not arguing that the obscured fraction has to be as low as $\sim 20\%$. Given the uncertainties (error bars in the observations, range of allowed Eddington ratio distributions and systematic uncertainty in our simple model of host properties), it could be somewhat (factor ~ 2) higher (as suggested by other independent constraints from e.g. infrared emission or X-ray background fitting; see e.g. Treister et al. 2008). What we show, however, is that simple effects could, within reasonable parameter space, account for up to $\sim 80\%$ of the claimed effects, in particular, the strong dependence on luminosity and redshift. In fact, direct observations

that do attempt to more rigorously distinguish obscured and unobscured sources in “complete” samples (e.g. narrow-line studies) favor a somewhat higher “true” obscured fraction $\sim 30 - 40\%$, but with a similar lack of luminosity and/or redshift dependence (see e.g. Hao et al. 2005a,b, and references therein).

Qualitatively similar observational results to those shown in Figure 4 on the fraction of obscured systems have been obtained by using X-ray hardness (rather than optical SEDs) as a proxy for obscuration; i.e. systems with sufficiently hard X-ray spectra are classified as obscured (although it should be noted, the statistics in these studies are much more limited). If real, this is difficult to explain with simple host galaxy dilution. However, in Figure 3, we noted that the expected RIAF spectra are similar in their X-ray hardness to a genuine obscured (intrinsically Type 1) SED. We consider this in more detail in the top panel of Figure 6, which shows the X-ray SEDs for Type 1, genuinely Type 2 dust/gas-obscured, pure RIAF, and RIAF+outer thin disk models. The RIAF SEDs are hard power laws; they do not have an absorption cutoff. But, if we ignore that cutoff, only seen at < 1 keV rest-frame, the RIAF SEDs

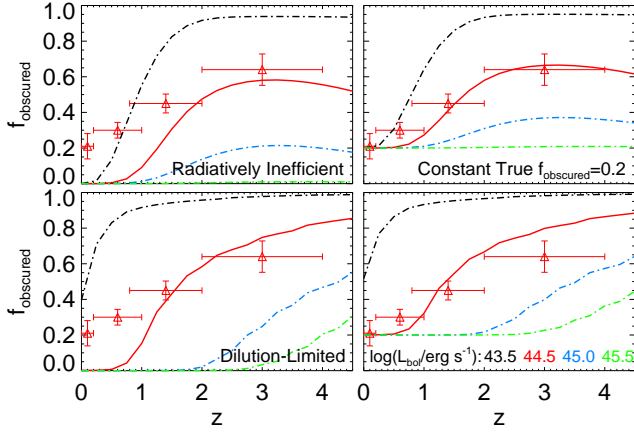


Figure 5. As in Figure 4, but plotting the predicted fraction that would appear “observed” in optical samples at a given L (as labeled) as a function of redshift. Also shown are the corresponding observational estimates from Hasinger (2008) for luminosities in the range $L \sim 10^{44} - 10^{45} \text{ erg s}^{-1}$.

are sufficiently hard that they are indistinguishable (with typical signal-to-noise) from the SED of the true obscured AGN; both are significantly harder than the SED of an unobscured AGN out to $> 10 \text{ keV}$.

To quantify the extent to which our theoretically calculated RIAF spectra could mimic obscuration, Figure 6 also shows the hardness ratio (HR) as a function of galaxy redshift for these template SEDs, with hardness ratio defined in terms of the observed-frame hard (2–10 keV) and soft (0.5–2 keV) band counts, $\text{HR} = (H - S)/(H + S)$.⁶ Larger absolute values of HR correspond to “harder” SEDs and, it is usually believed, a more obscured system.

The RIAF model, being a near power-law, predicts a constant, relatively hard HR. We compare this to the HR derived from the Type 1 template shown, obscured by different columns $N_H = 10^{22}, 10^{23}, 10^{24} \text{ erg s}^{-1}$. The template shown corresponds to an intrinsic photon index $\Gamma = 1.9$ (see Elvis et al. 1994; George et al. 1998; Perola et al. 2002; Ueda et al. 2003; Vignali et al. 2003), with a reflection component generated by the PEXRAV model (Magdziarz & Zdziarski 1995) following Ueda et al. (2003). We also show the results for varying Γ , within the range suggested by observations, $\Gamma = 1.8 - 2.0$ (dotted lines in the middle panel of Fig. 6).

At $z \gtrsim 1$, the strong absorption cutoff in true obscured systems is redshifted out of the soft band, and the hardness ratios from obscured systems are similar to the power-law spectra expected in RIAF models (middle panel; Fig. 6). We therefore consider what column densities would be inferred, if the true spectrum were the RIAF model observed at some redshift, but the observed hardness

⁶ Note that the observed hardness ratio, as defined in terms of counts, depends on the exact waveband and instrument response function. For the sake of generality, what we quote here can be thought of as an “intrinsic” HR for an instrument with perfect response and sensitivity, with fixed bands defined from 0.5 – 2.0 keV and 2.0 – 10.0 keV; as such, it is not directly comparable to hardness ratios in the literature for real instruments and wavebands. Because we are interested in comparing two input SEDs (the obscured AGN and RIAF), however, so long as we treat them identically it makes little difference to our conclusions whether we adopt this definition or model a more complex instrumental response function. There is, however, some weak sensitivity to the wavebands in which hardness ratios are defined, since these will sample various portions of the absorption cutoff at different redshifts.

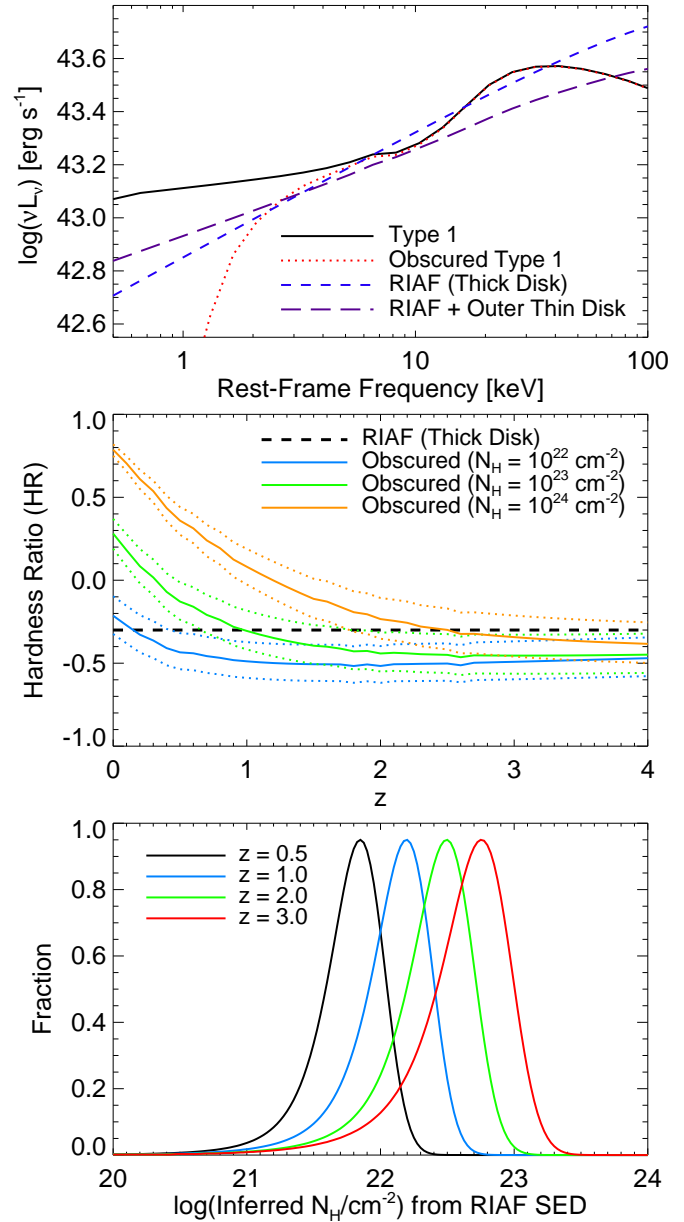


Figure 6. *Top:* Comparison of template AGN SEDs in the X-ray; we consider Type 1, obscured, pure RIAF, and RIAF+outer disk models. The RIAFs predict hard X-ray SEDs similar to an obscured system, but without a true absorption cutoff. *Middle:* Observed hardness ratio (HR) from the templates in the top panel as a function of redshift. The Type 1 template is obscured by different columns $N_H = 10^{22}, 10^{23}, 10^{24} \text{ erg s}^{-1}$ for input photon index $\Gamma = 1.9$ (solid lines) and Γ varying from 1.8 – 2.0 (dotted lines). At $z \gtrsim 1$, the strong absorption cutoff in true obscured systems is redshifted out of the soft band, and the hardness ratios from obscured systems are similar to the power-law spectra expected in RIAF models. *Bottom:* Inverting the *middle* plot: Given the template RIAF hardness, we plot the column density N_H that would be inferred by matching this hardness to an obscured Type-1 SED. We assume observational errors of ~ 0.1 in HR, comparable to deep observed X-ray samples (see Hasinger 2008).

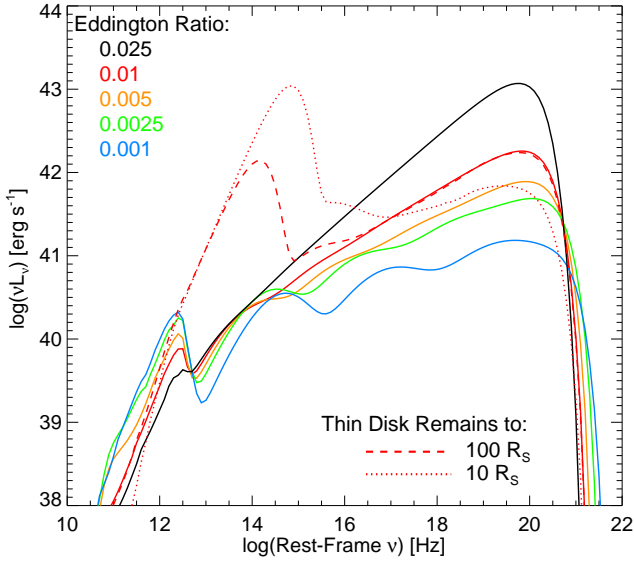


Figure 7. Model RIAF spectra at Eddington ratios $\dot{m} = 0.025, 0.01, 0.005, 0.0025, 0.001$ (solid; black, red, orange, green, blue, respectively, from top to bottom in the X-rays). Also shown are models with $\dot{m} = 0.01$ in which there is an outer thin disk that transitions to the inner RIAF at a radius of 10 (dotted) and 100 (dashed) Schwarzschild radii. For the simple comparisons made in this paper (“obscured” or “unobscured”), the differences between the different \dot{m} have little impact; the optical SEDs are always strongly suppressed, and the X-ray SEDs are power-law like (over $\sim 0.5 - 100$ keV) with similar hardness for the accretion rates of interest, down to very low- L ($L_{\text{bol}} \ll 10^{42}$ erg s $^{-1}$) where the spectra become softer.

ratio were modeled as the template Type 1 SED plus obscuration (allowing for typical errors in hardness ratio $\Delta HR \sim 0.1$, typical of the quality in deep X-ray samples). This is the common method for inferring obscuration in X-ray samples (e.g. Ueda et al. 2003; La Franca et al. 2005; Barger & Cowie 2005; Gilli et al. 2007); applied to a hard power-law like spectrum expected in radiatively inefficient states, it can lead to a significant false obscuration signal, with inferred column densities $N_H \sim 10^{22} - 10^{23}$ cm $^{-2}$ (bottom panel of Fig. 6). At these redshifts, observations are sampling the regime where the RIAF SEDs are significantly harder than that of an unobscured AGN, but missing the regime where the strong absorption cutoff distinguishing true absorption can be sampled.

Figure 7 shows how the RIAF spectrum varies as a function of accretion rate. As \dot{m} decreases, the predicted X-ray spectra become softer (a transition that has also been suggested from observed AGN; see e.g. Dai et al. 2004; Saez et al. 2008; Constantin et al. 2009); however, they are still harder than an unobscured AGN for all $\dot{m} \gtrsim 0.001$ (below which the luminosities are sufficiently low that they contribute negligibly to the different fixed-luminosity samples considered here). It therefore makes little difference whether we simply pick one of these Eddington ratios as “representative” of the RIAF SED, or include the full \dot{m} dependence in the predictions here. Changing other parameters in the model shown in Figure 7, such as the disk viscosity, the magnetic energy density (relevant for the predicted synchrotron emission), and mass loading of outflows does not significantly change the spectral shape at fixed \dot{m} . The strength of outflows is important for the normalization of the SED, i.e., for the ratio of the luminosity to the (large-scale) accretion rate, but at fixed luminosity makes little difference. In other words, although some of the details of RIAF accretion flows remain

uncertain, the vast majority of these issues do not affect our qualitative conclusions. RIAF SEDs are generally X-ray hard; this must be true, since they are designed to describe the observed “low/hard” (low-luminosity, hard X-ray spectrum) state in X-ray binaries. The dominant uncertainty for our purposes lies in the nature of the transition to the RIAF state. If this is more gradual than what we have assumed here – i.e. if a significant thin disk survives all the way down to small radii for Eddington ratios $\dot{m} < 0.01$, then the X-ray SED could be significantly softer (owing to inverse Compton cooling of the inner thick disk photons), although it must survive to very small radii indeed (only being an important effect if the transition radius is $\lesssim 10$ Schwarzschild radii). Of course, this is essentially equivalent to the uncertainty regarding whether such a transition occurs at all (see, for example, Maoz 2007).

It is also important to note, as is clear in Figure 6 that the RIAF SEDs do not become extremely hard. It is difficult, with such models and no true obscuration, to mimic e.g. Compton thick columns with $N_H > 10^{23}$ cm $^{-2}$. Ultimately, more detailed observational studies will allow direct comparison of the hardness ratio distribution at each redshift, which could include components that cannot be mimicked by RIAF models.

We now estimate the fraction of AGN that might be classified as “obscured” on the basis of observed X-ray hardness, as a consequence of having an intrinsic RIAF-type SED. This is shown in Figure 8 as a function of luminosity and redshift. The model is the same as in our predictions for optical samples, but we assume that all sources with $\dot{m} < 0.01$ have a thick disk spectrum as in Figure 3, and calculate the hardness ratio distribution and implied column density distribution as in Figure 6. As in the observational literature (e.g., Gilli et al. 2007 and references therein), we classify as “obscured” all sources with an inferred column $N_H > 10^{22}$ erg s $^{-1}$. The radiatively efficient ($\dot{m} > 0.01$) sources are assumed to be either uniformly unobscured (“true $f_{\text{obscured}} = 0$ ” case; left panel) or to have a constant fraction $f_{\text{obscured}} = 0.2$ of sources genuinely obscured (right panel). The resulting trends in obscured fraction as a function of luminosity and redshift are similar to those in Figures 4 & 5 (the optical samples). By taking into account the predicted change in AGN SEDs below $\dot{m} \simeq 0.01$, we thus conclude that a significant fraction of the inferred dependence of obscuration on luminosity/redshift, both determined from optical observations and X-ray hardness cuts, could owe to the fraction of systems in a radiatively inefficient state, rather than from true obscuration.

4 AGN CLUSTERING VERSUS SELECTION AND FUELING

By affecting the distribution of Eddington ratios detected in a given sample, dilution and radiative efficiency selection effects can also affect the BH masses to which the sample is sensitive, and thus stellar/host masses. Given the strong dependence of clustering on stellar/halo mass, the overall clustering amplitude measured in such a sample can be different than that inferred from a sample including all active systems.

Another important effect for observed clustering is related to the significant time systems can remain active after their initial peak of activity; if, after a near-Eddington peak in activity, the AGN accretion rate declines in an approximate power-law fashion $\propto (t/t_0)^{-\beta}$, then for a system at much lower Eddington ratio \dot{m} , it has been a time $\sim t_0 \dot{m}^{-1/\beta}$ since the peak of activity. For characteristic $t_0 \sim 10^8$ yr suggested by observational estimates of the AGN lifetime and $\beta \sim 1 - 3$ from a variety of different models (see

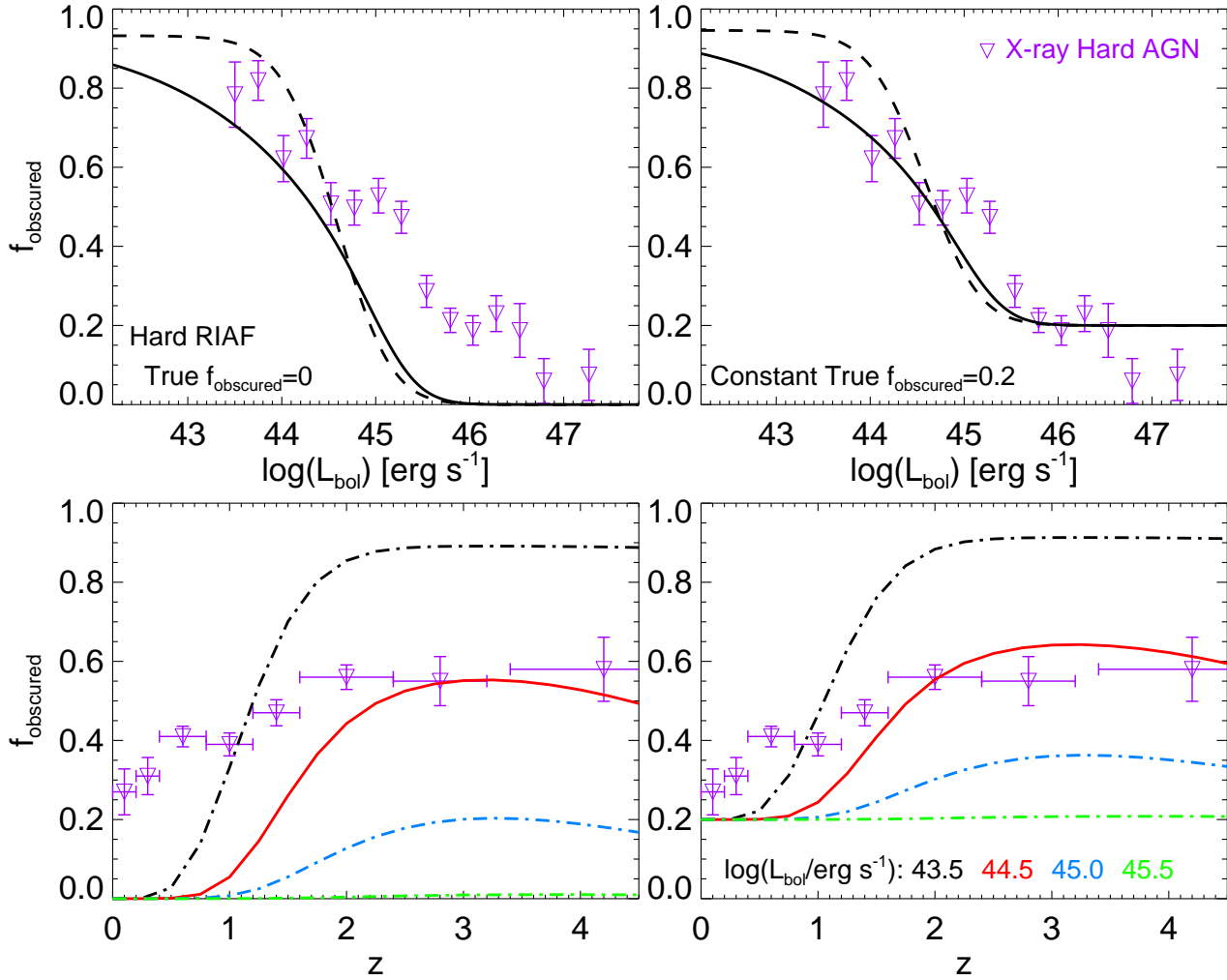


Figure 8. The fraction of systems that would be classified as “obscured” based on their observed X-ray hardness ratios (as shown in Figure 6 as a function of luminosity and redshift); we assume that for $\dot{m} < 0.01$, all accretion is via a RIAF. The predictions are compared with the observed fraction of hard X-ray sources, typically classified as “obscured” (Hasinger 2008). Because RIAFs have intrinsically hard spectra, X-ray hardness alone does not necessarily break the degeneracies between selection effects and true obscuration demonstrated in Figures 4-5. X-ray spectra with the sensitivity to measure the presence or absence of a true absorption cutoff are needed to definitively show obscuration.

Hopkins & Hernquist 2006, 2009, and references therein), this time is still small compared to the Hubble time for high Eddington ratios $\dot{m} \gtrsim 0.1$. The system is therefore viewed with no significant evolution in its properties between the peak of activity and the time at which it is observed. However, at sufficiently low Eddington ratios $\dot{m} \ll 0.01$, the initial trigger may have occurred at a much earlier time \gtrsim Gyr (comparable to a Hubble time), implying that systems observed at e.g. $z = 0$ – having decayed for Gyr down to these Eddington ratios – were active/forming at much earlier times, and therefore are more biased than a system of similar mass first becoming active at $z = 0$. Modeling this in detail requires a detailed and specific model for AGN lightcurves and triggering; we adopt the results from McQuinn et al. (2009) (see Hopkins et al. 2007a, 2008a, 2009, for more details) to demonstrate the effects here; however, many of the qualitative results are general. That model uses identical assumptions to the model described here in § 2 (the same AGN luminosity function, light curves, Eddington ratio and host property distributions), but places the mock AGN in halos in a cosmological simulation according to the observationally constrained galaxy mass-halo mass relations (see e.g. Moster et al. 2009, and

references therein), and so can predict clustering and other properties.

Figure 9 shows the bias as a function of luminosity taking into account the above effects and for our three different “observational” samples. At the bright end, there is no difference between models and a reasonably steep dependence of clustering on luminosity, because essentially all models agree that AGN must be near-Eddington at these luminosities, implying that the luminosity function is a sequence in BH/host mass. At luminosities $\lesssim L_*$, however, the fact that non-trivial lightcurves allow the population to be a mix of both high and low Eddington ratio systems rather than a strict sequence in mass makes the dependence of clustering amplitude on luminosity relatively weak, as is observed (Porciani et al. 2004; Adelberger & Steidel 2005; Porciani & Norberg 2006; Coil et al. 2007; da Angela et al. 2008) (for more details regarding the modeling of clustering, see Lidz et al. 2006). For “complete” samples, the clustering amplitude is predicted to *increase* at lower luminosities, because of an increasing contribution of very massive systems that have decayed to very faint luminosities (low Eddington ratios). Indeed, observations of faint X-ray sources appear to support

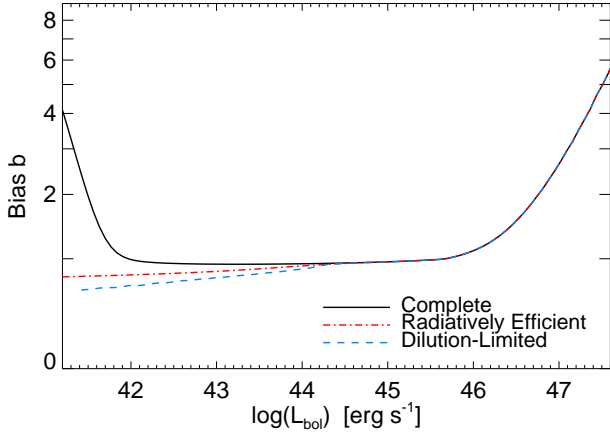


Figure 9. Dependence of clustering on luminosity at $z \sim 0$ for the different samples described in Figure 1. At $L \gtrsim L_*$, the samples are all similar, with mostly near-Eddington systems; thus L scales roughly with halo mass and there is a steep $b(L)$. At lower L , the broad range of Eddington ratios leads to a weak dependence of $b(L)$ and can cause differences in different samples (see Lidz et al. 2006). At very low L , the clustering in a complete sample can increase again (depending on the exact lightcurve/lifetime model), as the luminosity function can be dominated by early-forming highly clustered BHs that have had time to decay to very low luminosities. These low \dot{m} systems would not appear in radiatively efficient or dilution-limited samples.

this, with a surprisingly high clustering amplitude in several cases (see e.g. Constantin & Vogeley 2006; Plionis et al. 2008; Gilli et al. 2009; Hickox et al. 2009) – higher than observed in optical samples at the same redshift and similar or higher luminosities (Croom et al. 2005; Myers et al. 2007; da Angela et al. 2008).

If, however, these sources are selected against in optical/IR samples, then the clustering amplitude remains flat or decreases at low luminosities, reflecting the fact that the most biased sources (which are very massive, old galaxies that with AGN at very low Eddington ratios) are excluded, leaving a sample dominated by lower-mass systems at intermediate/high Eddington ratios. This may explain why the clustering amplitudes in X-ray and optical samples appear to disagree at low luminosities.

Figure 10 shows the clustering amplitude expected as a function of redshift for our standard three samples of AGN at two different intervals in bolometric luminosity. At a relatively high luminosity (top panel), which corresponds roughly to $\sim L_*$ in the AGN luminosity function over the redshift range $z \sim 0.5 - 2$ (see e.g. Hopkins et al. 2007b), the different selection methods yield nearly identical clustering amplitudes, in agreement with a variety of observations. At low luminosities, however ($L_{\text{bol}} \sim 10^{43} - 10^{44} \text{ erg s}^{-1}$, corresponding to $L_{2-10\text{keV}} \sim 10^{42} - 10^{43} \text{ erg s}^{-1}$), the bias versus redshift depends on the selection criteria (bottom panel in Fig. 10). In particular, at these luminosities, AGN selected in dilution-limited samples are preferentially at high Eddington ratio and therefore, smaller BHs in low-mass, weakly-clustered hosts. The bias as a function of redshift is somewhat sensitive to the exact model we adopt, but the selection effects are in any case clearly not negligible – they can lead to a factor of ~ 2 difference in bias, which corresponds to up to an order-of-magnitude difference in the implied host halo mass at these redshifts and bias values. This is qualitatively similar to what is observed in radio versus X-ray versus infrared-selected AGN samples (e.g., Hickox et al. 2009).

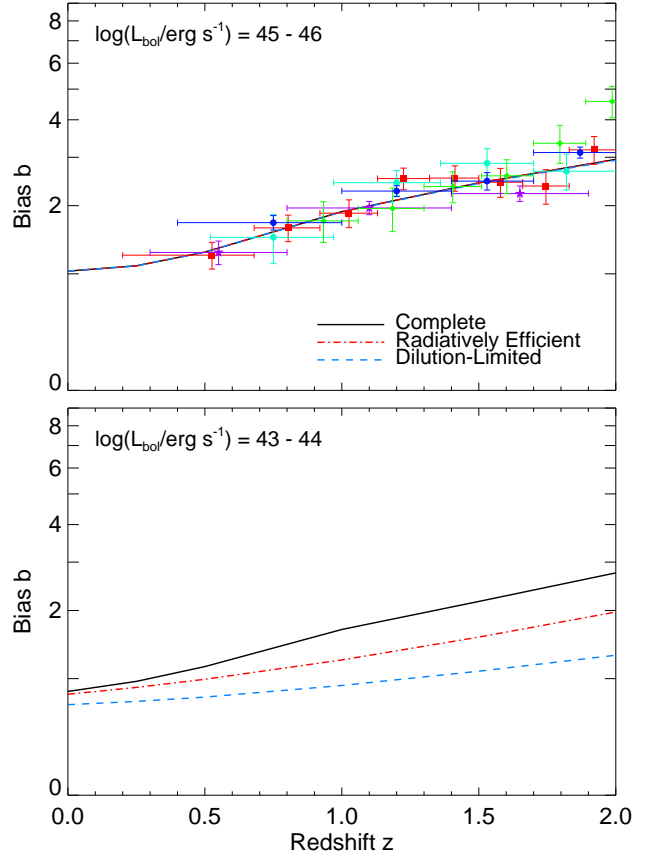


Figure 10. Dependence of AGN clustering on redshift in an intermediate-high luminosity sample ($\sim L_*$ quasars at these redshifts; *top*) and a low-luminosity sample (corresponding to $L_{2-10\text{keV}} \sim 10^{42} - 10^{43} \text{ erg s}^{-1}$ or $M_B \sim -17$; *bottom*), taking into account the different selection effects described in Figure 1. For the $\sim L_*$ sample, where most observations have been made, the different selection effects do not significantly change the predicted bias, which is also consistent with the observed clustering of quasars of similar luminosities from optically selected samples in Croom et al. (2005, red squares), Porciani & Norberg (2006, green diamonds), Myers et al. (2007, 2006, cyan and blue circles), and da Angela et al. (2008, violet stars). At very low luminosities, the effects described in Figure 9 and § 5 lead to significant differences between samples; the higher bias in X-ray samples has been observed in a number of studies (see text).

5 DIFFERENCES IN HOST MASSES AND MORPHOLOGIES

At a given luminosity, different Eddington ratios imply different BH masses and thus different host masses. Given the strong correlation between galaxy morphology and stellar mass, this naturally leads to variations in host morphologies found in different samples. Recall, our model includes both the host total mass and bulge/disk mass distributions. For convenience, we therefore adopt the bulge-to-total ratio B/T as our morphological proxy of interest.

Some caution is warranted here – making such a conversion implicitly assumes that whatever fuels objects is statistically random at each bulge mass/luminosity, and does not select out a specific morphological sub-population at a given stellar mass. This is not necessarily true if e.g. mergers or disk instabilities are the dominant means of AGN fueling. Nevertheless, some samples suggest that, at least at low luminosities where fueling an AGN requires only a small gas supply, the host distribution spans a wide range

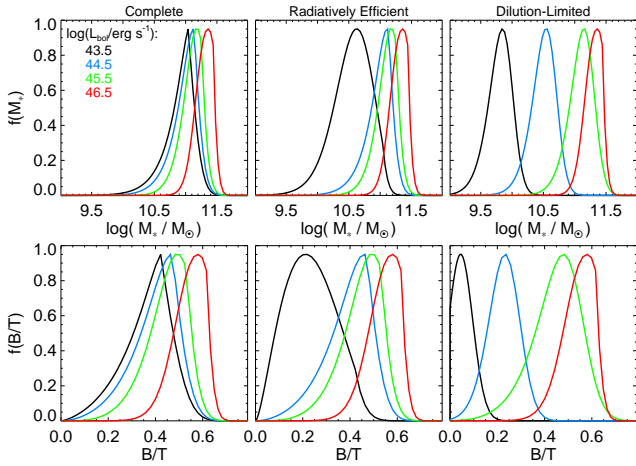


Figure 11. Model distribution of host galaxy stellar masses and B/T (bulge-to-total stellar mass ratio, our proxy for morphology) as a function of bolometric luminosity for the different selection samples considered in Figure 1. In a complete sample (X-ray or narrow line), even low- L AGN populations are dominated by relatively massive ($M \sim 10^{10.5} - 10^{11} M_\odot$) early-type (Sa/S0/E) hosts, as is observed (e.g. Kauffmann et al. 2003). In a radiatively efficient or dilution limited sample, however, the requirement of moderate Eddington ratios at low L leads to host masses and morphologies that are more luminosity-dependent: lower- L AGN in these samples will be hosted by lower-mass, late-type ($B/T \lesssim 0.3$) galaxies. This can explain the tension between the “conventional wisdom” that Seyferts live in disks (from optical-IR samples) and the contradictory results from recent narrow-line or X-ray samples that moderate-luminosity AGN have primarily early-type hosts.

and does not show a strong preference for specific morphological types (Bahcall et al. 1997; Malkan et al. 1998; Heckman et al. 2004; Falomo et al. 2004; Sánchez et al. 2004; Rigby et al. 2006; Nandra et al. 2007). At higher luminosities this is probably not the case, but as before, it is the low-luminosity regime where the Eddington ratio distribution is broad and has a significant effect.

The predicted host stellar mass and morphology distributions are shown in Figure 11. For the reasons discussed in § 4, a sample that includes objects of all types (including those that are radiatively inefficient or diluted in the optical/IR) is dominated by relatively massive ($\sim L_*$) early-type galaxies at all luminosities. This conclusion has been reached observationally in e.g. narrow line and deep X-ray samples: Kauffmann et al. (2003), Kewley et al. (2006) and Hao et al. (2005b) show that host luminosity and mass are nearly independent of AGN luminosity, with early-type morphologies predominant (similar to the X-ray conclusions discussed in Figure 2). However, in a sample with an implicit Eddington ratio selection, only low-mass BHs are present in the sample at low luminosities, which leads to a host sample dominated by less massive, more disk-dominated and star-forming host galaxies.

This result can potentially resolve long-standing discrepancies between different observations of AGN host galaxies, in samples that should select for similar AGN bolometric luminosities. We illustrate this in Figure 12, where we plot the median B/T as a function of AGN luminosity for two model samples: our complete sample and the dilution limited/optical broad-line sample (we do not plot host masses/luminosities because this information is already effectively presented in Figure 2, given $M_{\text{BH}} \propto M_{\text{bulge}}$; moreover the host morphology distribution is the primary focus of many studies attempting to constrain AGN fueling processes). We compare with roughly comparable observational samples: the deep narrow-

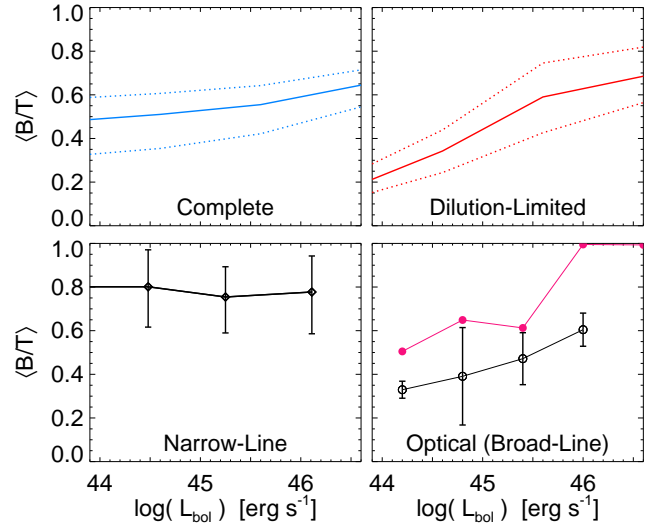


Figure 12. *Top:* Median bulge-to-total ratio as a function of luminosity, for the complete (*left*) and dilution-limited (*right*) samples in the model. Dotted lines show the $\pm 1\sigma$ range in the population. *Bottom Left:* Corresponding observational estimates from the narrow-line SDSS AGN sample (Kauffmann et al. 2003), converting L_{OIII} to bolometric and concentrations to B/T given the mean observed relation in Graham (2001) (error bars are the dispersion in the population, not errors in the median). *Bottom Right:* Same, based on the optically-selected PG quasar sample from Dunlop et al. (2003). We show the results both for their sample with “robust” morphologies (reliable bulge/disk decomposition; black circles) and their full sample (magenta squares).

line sample of Kauffmann et al. (2003) (which includes faint objects with luminosities well below those of their hosts) and the broad-line PG quasar sample (all of which have $L_{\text{AGN}} \gtrsim L_{\text{host}}$) from Dunlop et al. (2003) and Floyd et al. (2004).⁷

The “conventional wisdom,” derived from early faint AGN samples that were dominated by broad-band optical/UV color selection, has been that Seyferts reside predominantly in disk-dominated, low-mass galaxies (Adams 1977; Smith et al. 1986; Granato et al. 1993; McLeod & Rieke 1995); this is still true in modern samples that adopt similar selection methods, i.e., that require a moderate UV/optical/IR luminosity from the AGN relative to the host galaxy (see e.g. Martini & Pogge 1999; Peletier et al. 1999; Dunlop et al. 2003; Zakamska et al. 2006, and references therein). These inferences are consistent with our models for a sample with an effective minimum Eddington ratio. However, sufficiently deep narrow-line and X-ray surveys (“complete” surveys) find instead that the AGN host population is dominated by massive early-type galaxies, at all luminosities. At a given (similar) bolometric luminosity, these surveys suggest that the AGN host fraction rises steeply as a function of bulge mass, in contrast to the results from Type 1-sensitive surveys. As Figure 12 shows, both results follow naturally once one takes into account a broad intrinsic distribution of Eddington ratios and the observational selection effects highlighted throughout this paper.

⁷ Note that the fitting procedures for B/T in these samples differ from the calibration in Balcells et al. (2007) that we use for our predictions – therefore some systematic offsets are expected. The qualitative trends with mass are of primary interest here.

6 DISCUSSION AND CONCLUSIONS

We have demonstrated that, given a non-trivial Eddington ratio distribution, two simple effects will give rise to potentially important differences in the AGN populations selected by different observational criteria. Even if the physics of accretion were independent of \dot{m} , an AGN will inevitably be much less luminous than its host galaxy in a given band at sufficiently low Eddington ratio. Dilution is, of course, inevitable, and in most surveys AGN will be classified as “normal galaxies” if the AGN luminosity is less than that of the host. In the optical/IR, this happens at surprisingly high Eddington ratios, $\dot{m} \sim 0.01 - 0.1$, for most low-luminosity populations, which is why the effects of dilution can have such a significant impact on AGN surveys. Moreover, at low accretion rates $\dot{m} \lesssim 0.01$, AGN may transition to a radiatively inefficient state, in which the optical and infrared emission decline rapidly, and eventually the broad-line region may disappear entirely (see footnote 2 in §1 for more discussion of how the broad line emission disappears). Regardless of the specific spectral changes that may occur, the phenomenon of low-efficiency accretion is increasingly well-established and at low accretion rates populations of AGN with little to no broad-line emission appear (Ho 1999; Moran et al. 2000; Tran 2003; Nicastro et al. 2003; Brightman & Nandra 2008; Bianchi et al. 2008).

At high luminosities, observed systems are uniformly at relatively high Eddington ratios, and so it is unlikely that either dilution or radiative inefficiency is a significant issue. At low luminosities, however, the “true” Eddington ratio distribution of all AGN, as constrained by sufficiently deep narrow-line, X-ray, and radio surveys, is broad and extends to lower \dot{m} with decreasing bolometric luminosity (roughly as $\lambda = L_{\text{bol}}/L_{\text{Edd}} \propto L_{\text{bol}}^{0.5-1}$ at sufficiently low luminosities; see, e.g., Fiore et al. 2003; Silverman et al. 2005a; Hickox et al. 2009); this is consistent with some theoretical models of AGN lightcurve evolution (Hopkins & Hernquist 2009).

Given the selection effects implicit in the construction of a broad-line or Type 1 optical/mid-IR AGN sample, our results imply that dilution and radiative efficiency lead to these samples preferentially sampling the high- \dot{m} end of the population, with $\dot{m} \gtrsim 0.1$ and a relatively narrow range in \dot{m} even at low luminosities. This is indeed observed (Figures 1-2). The strong impact of selection criteria is illustrated by the distinct Eddington ratio distributions recovered in X-ray samples (where dilution is weak, and radiatively efficiency declines less rapidly) as compared to optical samples (compare Greene & Ho 2007).

For the same bolometric luminosity, different Eddington ratios imply different BH masses and, correspondingly, host galaxy masses. Low-luminosity AGN hosts in sufficiently deep narrow line/X-ray/“complete” samples should cluster around a narrow range in host mass, preferentially massive ($\sim L_*$), early-type galaxy hosts, as observed (Kauffmann et al. 2003; Hao et al. 2005a,b; Kewley et al. 2006; Silverman et al. 2008a; Hickox et al. 2009). However, low-luminosity AGN in dilution (or radiative efficiency)-limited samples will often be found in less massive hosts, which are correspondingly less bulge-dominated (Figures 11-12). This is also observed, and can reconcile conflicting claims in the literature regarding the hosts of Seyfert galaxies: samples based on optical/UV excess selection have traditionally found that these objects reside in less massive late-type disks (De Robertis et al. 1998; Martini & Pogge 1999; Knapen et al. 2000; Dunlop et al. 2003; Rigby et al. 2006) while more recent X-ray or narrow line surveys find that AGN preferentially lie in massive early type hosts (references above). As it is well-established that galaxies of different masses and morphologies cluster differently, these same ef-

fects also lead to differences in the expected clustering (Figure 9): faint X-ray/narrow-line/“complete” AGN samples should exhibit higher clustering amplitude than corresponding optical samples. This is consistently observed when comparing X-ray and optical/IR AGN clustering properties at low luminosities (see e.g. Porciani & Norberg 2006; Myers et al. 2007; Plionis et al. 2008, and references therein).

In most surveys, AGN are identified as “obscured” or “unobscured” in the optical based on a simple classification, namely whether the optical spectrum is dominated by a broad-line AGN SED or galaxy light; we have shown, however, that both dilution and radiative inefficiency will lead to the classification of an AGN as obscured (e.g., Fig. 3). The natural expectation is that the fraction of sources which are optically dim for these reasons should increase with decreasing luminosity. It is in fact traditionally inferred that the intrinsically “obscured” (non Type 1) AGN fraction behaves in just this manner (Hill et al. 1996; Willott et al. 2000; Steffen et al. 2003; Ueda et al. 2003; Grimes et al. 2004; Hasinger 2004; Sazonov & Revnivtsev 2004; Barger & Cowie 2005; Gilli et al. 2007; Hickox et al. 2007; Hasinger 2008). We find, however, that the fraction of AGN that are diluted (and may also be radiatively inefficient) scales in a similar manner to the observed optically “obscured” fraction, with both luminosity and redshift. The effect is not large enough to account for all optically dim objects (in particular at high L), but the fraction of “true” obscured sources could, in principle, be as low as $\sim 20 - 40\%$, with a much weaker dependence on both luminosity and redshift than that traditionally inferred (see Figures 4-8).

Using X-ray hardness as a measure of obscuration represents an improvement over the “optically dim” criterion in many ways (e.g., it should not be affected by simple dilution). However, the expected X-ray SEDs of AGN in radiatively inefficient states are relatively hard power-laws for $\dot{m} \sim 10^{-2}$ (Figure 7). They are sufficiently hard, in fact, that the systems would be classified as obscured/hard sources by the standard observational criterion – which uses a simple hardness ratio to probe the presence or absence of an absorption cutoff, given the lack of full X-ray spectra at the signal to noise ratios available for most high redshift sources. Convoluting with the observed Eddington ratio distribution, we find that RIAFs could explain a large fraction of the X-ray “obscured” sources at low luminosities ($L_{\text{bol}} \lesssim 10^{45} \text{ erg s}^{-1}$, or $L_{2-10 \text{ keV}} \lesssim 3 \times 10^{43} \text{ erg s}^{-1}$). In particular, just as with the optical samples, we find that the “true” obscured fraction could be as low as $\sim 20 - 40\%$, with a much weaker dependence on luminosity and/or redshift than has been suggested by observations based on hardness ratio distributions. It is important to stress that we are not questioning the fact that *local* samples of Seyferts indicate a large population of obscured sources. Rather we are pointing out that the hard X-ray spectra detected in higher redshift samples may in many cases be *intrinsic* (having to do with accretion physics), rather than indicative of absorption.

Consistent with the conclusions drawn here, detailed observations have revealed that dilution accounts for a significant fraction of the optically dim population at luminosities $L_{\text{bol}} \lesssim 10^{45} \text{ erg s}^{-1}$ (Moran et al. 2002; Hao et al. 2005b; Severgnini et al. 2003; Georgantopoulos & Georgakakis 2005; Georgakakis et al. 2006; Eckart et al. 2006; Garcet et al. 2007; Gruppioni et al. 2008). Specifically, a large fraction of the sources identified as Type 2 on the basis of a lack of observed broad lines or optical/IR AGN continuum do not show similar evidence for obscuration based on X-ray followup (see e.g. Akylas et al. 2006; Caccianiga et al. 2008; Hasinger 2008). In many optical/IR studies the Type 2 frac-

tion remains as high as $f_{\text{obscured}} \sim 0.6 - 0.7$ up to luminosities $L_{\text{bol}} \lesssim 3 \times 10^{45} \text{ erg s}^{-1}$ ($L_{2-10\text{keV}} \lesssim 10^{44} \text{ erg s}^{-1}$), by which point the obscured fraction suggested by X-ray followup has dropped to $f_{\text{obscured}} \sim 0.2$ (see also Tajer et al. 2007); Della Ceca et al. (2004) and Caccianiga et al. (2007), for example, find that this corresponds closely to what is seen in deeper follow-up of X-ray selected and apparently optically dim sources in the XMM-Newton survey. Hao et al. (2005b) estimate from a narrow-line (SDSS galaxy) sample that the true obscured fraction remains a constant $\sim 30 - 40\%$ from luminosities $L_{\text{bol}} \sim 10^{42} - 10^{45} \text{ erg s}^{-1}$ ($L_{\text{OIII}} \sim 10^5 - 10^8 L_{\odot}$). Thus $\sim 50 - 80\%$ of the claimed obscured sources in this luminosity range (above $L_{\text{bol}} \sim 10^{44} \text{ erg s}^{-1}$ or $L_{2-10\text{keV}} \sim 10^{42} \text{ erg s}^{-1}$) appear to simply be diluted.

Note that, although we have found that the obscured fraction could be as low as $\sim 20\%$, we are not strongly advocating this specific number; this low constant level of obscuration (relatively independent of luminosity and redshift) corresponds to the maximum effect of dilution on observational surveys, given the uncertainties in our approach and the observations. The observational studies above suggest that the true baseline obscured fraction may be $\sim 30 - 40\%$ or even slightly higher. Our key point is that the observed *trend* of obscuration with luminosity is very sensitive to dilution. And although it has been well appreciated that dilution can significantly affect low luminosity AGN samples selected in the optical/IR, it has not been as widely appreciated that it also biases the inferred Eddington ratios, host mass and morphology distributions, and even clustering amplitudes (as we have demonstrated). Moreover it is not clear whether any trivial “correction” can be applied to these samples to correct for these effects.

More detailed observations probing the type of systems we appeal to here are clearly important. Unfortunately, they are also difficult. As noted above, the sources of interest – those that may dominate the “obscured”/hard population at low luminosities in large X-ray surveys – are *not* analogous to well-studied local Seyfert 2 galaxies (which are indeed obscured by dust and gas). The latter are primarily nearby, relatively active systems in low-mass, star-forming and/or disky host galaxies. In contrast, the optically dim/hard population that dominates at low luminosities in large X-ray surveys contains a large fraction of massive elliptical galaxies ($M_* \gtrsim 10^{11} M_{\odot}$, and BH mass $\sim 10^8 - 10^9 M_{\odot}$) firmly in the “red sequence” (i.e. without star formation or significant gas content), with low Eddington ratios $\lambda \sim 10^{-3} - 10^{-2}$, and relatively high clustering amplitudes (see e.g. Figures 2-12 and Fiore et al. 2003; Kauffmann et al. 2003; Brand et al. 2005; Nandra et al. 2007; Silverman et al. 2008a; Hickox et al. 2009). In some ways this population is more analogous to radio galaxies (but many of the systems of interest are still radio-quiet), for which a number of models and observations suggest that low Eddington ratios and differences in accretion physics (relative to local Seyferts) are important (Smith et al. 1986; Falcke & Biermann 1996; Meier 2001; Ho 2002; Maccarone et al. 2003; Best et al. 2007; Fender et al. 2007; Merloni & Heinz 2008).

A $L_{\text{bol}} \sim 10^{44} \text{ erg s}^{-1}$ BH in the radiatively inefficient regime (with $\lambda = L_{\text{bol}}/L_{\text{Edd}} \sim 0.001$ for $\dot{m} < 0.01$) implies a $\gtrsim 10^9 M_{\odot}$ BH, and there are only a few such objects within $\sim 100 \text{ Mpc}$. Interestingly, of the six such objects in the local volume with well-measured BH masses (from Tremaine et al. 2002; Marconi & Hunt 2003; Häring & Rix 2004), at least four (M87, NGC 1399, NGC 4649, and IC 1459) are considered RIAF candidates (albeit with some debate; and in e.g. the case of M87 the presence of a jet complicates comparisons; Sambruna et al. 1999; Di Matteo et al. 2000; Allen et al. 2000; Sulkanen & Bregman

2001; Fabbiano et al. 2003); they have luminosities $L_X \sim 10^{40} - 10^{43} \text{ erg s}^{-1}$ ($L_{\text{bol}} \sim 10^{41} - 3 \times 10^{44} \text{ erg s}^{-1}$) and extremely hard, power law-like X-ray SEDs (effective photon indices $\Gamma = 0.7 - 1.4$). These systems are distinct from many better-studied nearby Seyferts in low-mass galaxies, which have softer X-ray spectra $\Gamma \sim 2$ and Eddington ratios $\sim 10^{-2}$. These are small number statistics, but we reach similar conclusions if we consider the \sim dozen nearby BHs down to $\sim \text{few} \times 10^8 M_{\odot}$ (see Evans et al. 2005; Soria et al. 2006a,b; Ellis & O’Sullivan 2006; González-Martín et al. 2006). Generalizing from this very small sample, if $\sim 1/2$ of $M_{\text{BH}} \gtrsim 10^9 M_{\odot}$ BHs are active in this luminosity range with X-ray SEDs as hard as observed in this subset, this is already sufficient to account for $> 50\%$ of the observed hard X-ray (apparently “obscured”) population at these luminosities in large samples from $z \sim 0 - 1$. But deep studies searching for e.g. polarized thin-disk signatures could set clear lower limits on the fraction of such sources with “traditional” obscuration. Clearly, more detailed observations of the (admittedly small number of) local analogues is critical to inform our speculation that these systems may contribute significantly in large surveys.

There has been considerable debate about the exact physics dominant at low Eddington ratios (e.g., an ADAF, a jet-dominated spectrum, or some other RIAF model; see, e.g., Guainazzi et al. 2000; Angelini et al. 2001; Loewenstein et al. 2001; Lumsden et al. 2004; Gallo et al. 2006; Gliozzi et al. 2007; Ghosh et al. 2007; Brightman & Nandra 2008). We stress that we are not attempting to advocate any *specific* model among these. Rather, the key question is to test is whether the lack of optical emission and the hard X-ray spectra are intrinsic or the result of a large column, or even whether or not the X-ray data supports the optical conclusions (or whether those can be entirely accounted for by dilution). To do so, more observations to break the degeneracies between accretion state, dilution, and genuine obscuration are clearly important. Ideally, high-resolution nuclear optical and X-ray spectroscopy and optical polarimetry could be applied, as in the most well-studied local Seyferts, to break the degeneracies between these possibilities and the most popular alternatives (“receding torus” models, in which a circumnuclear torus leads to geometric obscuration at all luminosities, but with a luminosity-dependent covering angle). Although these observational tests may be possible for the local analogues noted above, most systems at these low luminosities in large surveys cannot be studied in such detail. Observations must instead rely on indirect probes; these probes do, however, allow statistical tests that are not possible in the small local populations, and the application of integral arguments following BH demographics (see e.g. Brand et al. 2005).

Perhaps the largest theoretical uncertainty in estimating the importance of radiatively inefficient accretion for large AGN samples is the rapidity of the transition from a thin disk to a RIAF. If the luminosity declines too rapidly in all bands, say, then all objects below some \dot{m} will simply drop out of all samples, and will not introduce significant differences between AGN samples in various wavelengths. If, on the other hand, the thin/thick transition occurs very slowly with decreasing \dot{m} , then the SEDs will remain relatively X-ray soft and optically/IR bright at lower luminosities (Fig. 7), leading to less of a contribution from such sources to the X-ray hard/optically dim populations. Constraints on the contribution of such sources to faint “obscured” AGN samples, therefore, are a potentially new and powerful way to determine in detail how (and indeed whether or not) AGN behavior changes at low accretion rates.

If dilution and radiative inefficiency are indeed significant

at the levels estimated here, they can naturally account for observed differences in AGN populations selected at various wavelengths and via different techniques. The apparently contradictory host galaxy properties, clustering, and Eddington ratio distributions from different samples can, in fact, be reconciled and understood using a coherent theoretical framework. The importance these effects for large AGN samples is also intimately related to the problem of AGN fueling. Black holes that gained most of their mass in early, high-accretion rate episodes and have since decayed to low luminosities over a Hubble time – typical in merger-driven fueling scenarios – may show up as low- \dot{m} populations in massive, early-type hosts. On the other hand, systems that continuously or stochastically fueled – expected in scenarios where BHs are fueled at lower levels by e.g. stellar winds or bars in disk galaxies – will plausibly show up as higher- \dot{m} populations in intermediate mass, later-type hosts.

The results highlighted here also represent an important revision and caveat to the unified model of AGN. Even if AGN physics are perfectly self-similar, dilution implies that objects selected in optical, infrared, or X-ray samples are *not* random subsets of the same parent population (with just viewing angle differences). Rather, dilution leads to host galaxy-dependent selection effects, biasing e.g. the Eddington ratio distribution, host luminosity/mass/age/clustering distributions, and other properties. Moreover, radiatively inefficient populations could represent a large fraction of the “obscured” population at low luminosities. This should not be viewed as a limitation of these observations – rather, it presents the opportunity for multiwavelength comparisons to develop new constraints on AGN fueling mechanisms, feedback, and host populations. Since AGN selection may not be strictly independent of host properties at low luminosities, comparison of the demographics selected in different wavelengths can break degeneracies between different fueling and host evolution models.

ACKNOWLEDGMENTS

We thank Paul Martini and Smita Mathur for helpful discussions. We also thank the anonymous referee for valuable comments and suggestions. This work was supported in part by NSF grants ACI 96-19019, AST 00-71019, AST 02-06299, and AST 03-07690, and NASA ATP grants NAG5-12140, NAG5-13292, and NAG5-13381. Support for PFH was provided by the Miller Institute for Basic Research in Science, University of California Berkeley. E.Q. is supported in part by NASA grant NNG06GI68G and the David and Lucile Packard Foundation.

REFERENCES

- Adams, T. F. 1977, *ApJS*, 33, 19
 Adelberger, K. L., & Steidel, C. C. 2005, *ApJ*, 630, 50
 Akylas, A., Georgantopoulos, I., Georgakakis, A., Kitsionas, S., & Hatziminaoglou, E. 2006, *A&A*, 459, 693
 Allen, S. W., Di Matteo, T., & Fabian, A. C. 2000, *MNRAS*, 311, 493
 Angelini, L., Loewenstein, M., & Mushotzky, R. F. 2001, *ApJL*, 557, L35
 Bahcall, J. N., Kirhakos, S., Saxe, D. H., & Schneider, D. P. 1997, *ApJ*, 479, 642
 Balcells, M., Graham, A. W., & Peletier, R. F. 2007, *ApJ*, 665, 1104
 Barger, A. J., & Cowie, L. L. 2005, *ApJ*, 635, 115
 Barger, A. J., Cowie, L. L., Mushotzky, R. F., Yang, Y., Wang, W.-H., Steffen, A. T., & Capak, P. 2005, *AJ*, 129, 578
 Bell, E. F., & de Jong, R. S. 2000, *MNRAS*, 312, 497
 Bell, E. F., McIntosh, D. H., Katz, N., & Weinberg, M. D. 2003, *ApJS*, 149, 289
 Best, P. N., von der Linden, A., Kauffmann, G., Heckman, T. M., & Kaiser, C. R. 2007, *MNRAS*, 379, 894
 Bianchi, S., Corral, A., Panessa, F., Barcons, X., Matt, G., Bassani, L., Carrera, F. J., & Jiménez-Bailón, E. 2008, *MNRAS*, 385, 195
 Blandford, R. D., & Begelman, M. C. 1999, *MNRAS*, 303, L1
 Brand, K., et al. 2005, *ApJ*, 626, 723
 Brightman, M., & Nandra, K. 2008, *MNRAS*, 390, 1241
 Bruzual, G., & Charlot, S. 2003, *MNRAS*, 344, 1000
 Caccianiga, A., Severgnini, P., Della Ceca, R., Maccacaro, T., Carrera, F. J., & Page, M. J. 2007, *A&A*, 470, 557
 Caccianiga, A., et al. 2008, *A&A*, 477, 735
 Cao, X., & Xu, Y.-D. 2007, *MNRAS*, 377, 425
 Ciotti, L., & Ostriker, J. P. 2007, *ApJ*, 665, 1038
 Ciotti, L., Ostriker, J. P., & Proga, D. 2009, *ApJ*, 699, 89
 Coil, A. L., Hennawi, J. F., Newman, J. A., Cooper, M. C., & Davis, M. 2007, *ApJ*, 654, 115
 Conroy, C., & Wechsler, R. H. 2009, *ApJ*, 696, 620
 Constantin, A., & Vogeley, M. S. 2006, *ApJ*, 650, 727
 Constantin, A., et al. 2009, *ApJ*, in preparation
 Croom, S. M., Boyle, B. J., Shanks, T., Smith, R. J., Miller, L., Outram, P. J., Loaring, N. S., Hoyle, F., & da Ângela, J. 2005, *MNRAS*, 356, 415
 da Ângela, J., et al. 2008, *MNRAS*, 383, 565
 Dai, X., Chartas, G., Eracleous, M., & Garmire, G. P. 2004, *ApJ*, 605, 45
 De Robertis, M. M., Yee, H. K. C., & Hayhoe, K. 1998, *ApJ*, 496, 93
 Della Ceca, R., et al. 2004, *A&A*, 428, 383
 Di Matteo, T., Colberg, J., Springel, V., Hernquist, L., & Sijacki, D. 2008, *ApJ*, 676, 33
 Di Matteo, T., Croft, R. A. C., Springel, V., & Hernquist, L. 2003, *ApJ*, 593, 56
 Di Matteo, T., Quataert, E., Allen, S. W., Narayan, R., & Fabian, A. C. 2000, *MNRAS*, 311, 507
 Di Matteo, T., Springel, V., & Hernquist, L. 2005, *Nature*, 433, 604
 Dunlop, J. S., McLure, R. J., Kukula, M. J., Baum, S. A., O’Dea, C. P., & Hughes, D. H. 2003, *MNRAS*, 340, 1095
 Eckart, M. E., Stern, D., Helfand, D. J., Harrison, F. A., Mao, P. H., & Yost, S. A. 2006, *ApJS*, 165, 19
 Ellis, S. C., & O’Sullivan, E. 2006, *MNRAS*, 367, 627
 Elvis, M., et al. 1994, *ApJS*, 95, 1
 Esin, A. A., McClintock, J. E., & Narayan, R. 1997, *ApJ*, 489, 865
 Evans, D. A., Hardcastle, M. J., Croston, J. H., Worrall, D. M., & Birkinshaw, M. 2005, *MNRAS*, 359, 363
 Fabbiano, G., Elvis, M., Markoff, S., Siemiginowska, A., Pellegrini, S., Zezas, A., Nicastro, F., Trinchieri, G., & McDowell, J. 2003, *ApJ*, 588, 175
 Falcke, H., & Biermann, P. L. 1996, *A&A*, 308, 321
 Falomo, R., Kotilainen, J. K., Pagani, C., Scarpa, R., & Treves, A. 2004, *ApJ*, 604, 495
 Fender, R., Koerding, E., Belloni, T., Uttley, P., McHardy, I., & Tzioumis, T. 2007, *ArXiv e-prints*, in press, arXiv:0706.3838, 706
 Fine, S., et al. 2008, *MNRAS*, 390, 1413

- Fiore, F., et al. 2003, *A&A*, 409, 79
- Floyd, D. J. E., Kukula, M. J., Dunlop, J. S., McLure, R. J., Miller, L., Percival, W. J., Baum, S. A., & O’Dea, C. P. 2004, *MNRAS*, 355, 196
- Gallo, L. C., Lehmann, I., Pietsch, W., Boller, T., Brinkmann, W., Friedrich, P., & Grupe, D. 2006, *MNRAS*, 365, 688
- Garcet, O., et al. 2007, *A&A*, 474, 473
- Georgakakis, A. E., Georgantopoulos, I., & Akylas, A. 2006, *MNRAS*, 366, 171
- Georgantopoulos, I., & Georgakakis, A. 2005, *MNRAS*, 358, 131
- George, I. M., Turner, T. J., Netzer, H., Nandra, K., Mushotzky, R. F., & Yaqoob, T. 1998, *ApJS*, 114, 73
- Ghosh, H., Pogge, R. W., Mathur, S., Martini, P., & Shields, J. C. 2007, *ApJ*, 656, 105
- Gilli, R., Comastri, A., & Hasinger, G. 2007, *A&A*, 463, 79
- Gilli, R., et al. 2009, *A&A*, 494, 33
- Gliozzi, M., Sambruna, R. M., & Foschini, L. 2007, *ApJ*, 662, 878
- González-Martín, O., Masegosa, J., Márquez, I., Guerrero, M. A., & Dultzin-Hacyan, D. 2006, *A&A*, 460, 45
- Graham, A. W. 2001, *AJ*, 121, 820
- Granato, G. L., De Zotti, G., Silva, L., Bressan, A., & Danese, L. 2004, *ApJ*, 600, 580
- Granato, G. L., Zitelli, V., Bonoli, F., Danese, L., Bonoli, C., & Delpino, F. 1993, *ApJS*, 89, 35
- Greene, J. E., & Ho, L. C. 2007, *ApJ*, 667, 131
- Grimes, J. A., Rawlings, S., & Willott, C. J. 2004, *MNRAS*, 349, 503
- Gruppioni, C., et al. 2008, *ApJ*, 684, 136
- Guainazzi, M., Oosterbroek, T., Antonelli, L. A., & Matt, G. 2000, *A&A*, 364, L80
- Hao, L., et al. 2005a, *AJ*, 129, 1783
- . 2005b, *AJ*, 129, 1795
- Häring, N., & Rix, H.-W. 2004, *ApJL*, 604, L89
- Hasinger, G. 2004, *Nuclear Physics B Proceedings Supplements*, 132, 86
- . 2008, *A&A*, 490, 905
- Heckman, T. M., Kauffmann, G., Brinchmann, J., Charlot, S., Tremonti, C., & White, S. D. M. 2004, *ApJ*, 613, 109
- Hickox, R. C., et al. 2007, *ApJ*, 671, 1365
- . 2009, *ApJ*, 696, 891
- Hill, G. J., Goodrich, R. W., & Depoy, D. L. 1996, *ApJ*, 462, 163
- Ho, L. C. 1999, *ApJ*, 516, 672
- . 2002, *ApJ*, 564, 120
- Hopkins, P. F., Cox, T. J., & Hernquist, L. 2008a, *ApJ*, 689, 17
- Hopkins, P. F., & Hernquist, L. 2006, *ApJS*, 166, 1
- . 2009, *ApJ*, 698, 1550
- Hopkins, P. F., Hernquist, L., Cox, T. J., Di Matteo, T., Martini, P., Robertson, B., & Springel, V. 2005a, *ApJ*, 630, 705
- Hopkins, P. F., Hernquist, L., Cox, T. J., Di Matteo, T., Robertson, B., & Springel, V. 2005b, *ApJ*, 630, 716
- . 2005c, *ApJ*, 632, 81
- . 2006a, *ApJS*, 163, 1
- Hopkins, P. F., Hernquist, L., Cox, T. J., & Kereš, D. 2008b, *ApJS*, 175, 356
- Hopkins, P. F., Hernquist, L., Cox, T. J., Kereš, D., & Wuyts, S. 2009, *ApJ*, 691, 1424
- Hopkins, P. F., Hernquist, L., Cox, T. J., Robertson, B., Di Matteo, T., & Springel, V. 2006b, *ApJ*, 639, 700
- Hopkins, P. F., Hernquist, L., Martini, P., Cox, T. J., Robertson, B., Di Matteo, T., & Springel, V. 2005d, *ApJL*, 625, L71
- Hopkins, P. F., Lidz, A., Hernquist, L., Coil, A. L., Myers, A. D., Cox, T. J., & Spergel, D. N. 2007a, *ApJ*, 662, 110
- Hopkins, P. F., Narayan, R., & Hernquist, L. 2006c, *ApJ*, 643, 641
- Hopkins, P. F., Richards, G. T., & Hernquist, L. 2007b, *ApJ*, 654, 731
- Ilbert, O., et al. 2009, *ApJ*, in press, arXiv:0903.0102
- Jahnke, K., Kuhlbrodt, B., & Wisotzki, L. 2004, *MNRAS*, 352, 399
- Jahnke, K., Wisotzki, L., Courbin, F., & Letawe, G. 2007, *MNRAS*, 364
- Jahnke, K., Wisotzki, L., & Sánchez, S. F. 2006, *New Astronomy Review*, 50, 766
- Jester, S. 2005, *ApJ*, 625, 667
- Jogee, S. 2006, in *Lecture Notes in Physics*, Berlin Springer Verlag, Vol. 693, *Physics of Active Galactic Nuclei at all Scales*, ed. D. Alloin, 143–+
- Kassin, S. A., et al. 2007, *ApJL*, 660, L35
- Kauffmann, G., & Heckman, T. M. 2008, *MNRAS*, in press, arXiv:0812.1224
- Kauffmann, G., et al. 2003, *MNRAS*, 346, 1055
- Kewley, L. J., Groves, B., Kauffmann, G., & Heckman, T. 2006, *MNRAS*, 372, 961
- Knapen, J. H., Shlosman, I., & Peletier, R. F. 2000, *ApJ*, 529, 93
- Kollmeier, J. A., et al. 2006, *ApJ*, 648, 128
- Kormendy, J., & Richstone, D. 1995, *ARA&A*, 33, 581
- La Franca, F., et al. 2005, *ApJ*, 635, 864
- Laor, A., Fiore, F., Elvis, M., Wilkes, B. J., & McDowell, J. C. 1997, *ApJ*, 477, 93
- Lapi, A., Shankar, F., Mao, J., Granato, G. L., Silva, L., De Zotti, G., & Danese, L. 2006, *ApJ*, 650, 42
- Lidz, A., Hopkins, P. F., Cox, T. J., Hernquist, L., & Robertson, B. 2006, *ApJ*, 641, 41
- Loewenstein, M., Mushotzky, R. F., Angelini, L., Arnaud, K. A., & Quataert, E. 2001, *ApJL*, 555, L21
- Lumsden, S. L., Alexander, D. M., & Hough, J. H. 2004, *MNRAS*, 348, 1451
- Maccarone, T. J., Gallo, E., & Fender, R. 2003, *MNRAS*, 345, L19
- Magdziarz, P., & Zdziarski, A. A. 1995, *MNRAS*, 273, 837
- Magorrian, J., et al. 1998, *AJ*, 115, 2285
- Malkan, M. A., Gorjian, V., & Tam, R. 1998, *ApJS*, 117, 25
- Maoz, D. 2007, *MNRAS*, 377, 1696
- Marchesini, D., Celotti, A., & Ferrarese, L. 2004, *MNRAS*, 351, 733
- Marconi, A., & Hunt, L. K. 2003, *ApJL*, 589, L21
- Martini, P. 2004, in *Coevolution of Black Holes and Galaxies*, ed. L. C. C. U. P. Ho, 169
- Martini, P., & Pogge, R. W. 1999, *Astron. J.*, 118, 2646
- McClintock, J. E., & Remillard, R. A. 2006, *Black hole binaries, In Compact stellar X-ray sources*. Edited by Walter Lewin & Michiel van der Klis, Vol. Cambridge Astrophysics Series, No. 39. (Cambridge, UK: Cambridge University Press), 157–213
- McLeod, K. K., & Rieke, G. H. 1995, *ApJ*, 441, 96
- McQuinn, M., Lidz, A., Zaldarriaga, M., Hernquist, L., Hopkins, P. F., Dutta, S., & Faucher-Giguère, C.-A. 2009, *ApJ*, 694, 842
- Meier, D. L. 2001, *ApJL*, 548, L9
- Menci, N., Cavaliere, A., Fontana, A., Giallongo, E., Poli, F., & Vittorini, V. 2003, *ApJL*, 587, L63
- Merloni, A., & Heinz, S. 2008, *MNRAS*, 388, 1011
- Moran, E. C., Barth, A. J., Kay, L. E., & Filippenko, A. V. 2000, *ApJL*, 540, L73
- Moran, E. C., Filippenko, A. V., & Chornock, R. 2002, *ApJL*, 579, L71
- Morrison, R., & McCammon, D. 1983, *ApJ*, 270, 119

- Moster, B. P., Somerville, R. S., Maulbetsch, C., van den Bosch, F. C., Maccio', A. V., Naab, T., & Oser, L. 2009, *ApJ*, in press, arXiv:0903.4682 [astro-ph]
- Myers, A. D., Brunner, R. J., Nichol, R. C., Richards, G. T., Schneider, D. P., & Bahcall, N. A. 2007, *ApJ*, 658, 85
- Myers, A. D., et al. 2006, *ApJ*, 638, 622
- Nandra, K., et al. 2007, *ApJL*, 660, L11
- Narayan, R., & Yi, I. 1994, *ApJL*, 428, L13
- Narayan, R., Yi, I., & Mahadevan, R. 1996, *A&AS*, 120, C287+
- Nicastro, F., Martocchia, A., & Matt, G. 2003, *ApJL*, 589, L13
- Pei, Y. C. 1992, *ApJ*, 395, 130
- Peletier, R. F., Knapen, J. H., Shlosman, I., Pérez-Ramírez, D., Nadeau, D., Doyon, R., Rodríguez Espinosa, J. M., & Pérez García, A. M. 1999, *ApJS*, 125, 363
- Peng, C. Y., Impey, C. D., Rix, H.-W., Kochanek, C. S., Keeton, C. R., Falco, E. E., Lehár, J., & McLeod, B. A. 2006, *ApJ*, 649, 616
- Perola, G. C., Matt, G., Cappi, M., Fiore, F., Guainazzi, M., Maraschi, L., Petrucci, P. O., & Piro, L. 2002, *A&A*, 389, 802
- Plionis, M., Rovilos, M., Basilakos, S., Georgantopoulos, I., & Bauer, F. 2008, *ApJL*, 674, L5
- Porciani, C., Magliocchetti, M., & Norberg, P. 2004, *MNRAS*, 355, 1010
- Porciani, C., & Norberg, P. 2006, *MNRAS*, 371, 1824
- Quataert, E., di Matteo, T., Narayan, R., & Ho, L. C. 1999, *ApJL*, 525, L89
- Quataert, E., & Narayan, R. 1999, *ApJ*, 520, 298
- Richards, G. T., et al. 2006, *ApJS*, 166, 470
- Rigby, J. R., Rieke, G. H., Donley, J. L., Alonso-Herrero, A., & Pérez-González, P. G. 2006, *ApJ*, 645, 115
- Saez, C., Chartas, G., Brandt, W. N., Lehmer, B. D., Bauer, F. E., Dai, X., & Garmire, G. P. 2008, *AJ*, 135, 1505
- Salpeter, E. E. 1955, *ApJ*, 121, 161
- . 1964, *ApJ*, 140, 796
- Sambruna, R. M., Eracleous, M., & Mushotzky, R. F. 1999, *ApJ*, 526, 60
- Sánchez, S. F., et al. 2004, *ApJ*, 614, 586
- Sazonov, S. Y., Ostriker, J. P., & Sunyaev, R. A. 2004, *MNRAS*, 347, 144
- Sazonov, S. Y., & Revnivtsev, M. G. 2004, *A&A*, 423, 469
- Severgnini, P., et al. 2003, *A&A*, 406, 483
- Shakura, N. I., & Sunyaev, R. A. 1973, *A&A*, 24, 337
- Shankar, F., Weinberg, D. H., & Miralda-Escudé, J. 2009, *ApJ*, 690, 20
- Sharma, P., Quataert, E., Hammett, G. W., & Stone, J. M. 2007, *ApJ*, 667, 714
- Sijacki, D., Springel, V., di Matteo, T., & Hernquist, L. 2007, *MNRAS*, 380, 877
- Silverman, J. D., et al. 2005a, *ApJ*, 624, 630
- . 2005b, *ApJ*, 618, 123
- . 2008a, *ApJ*, 675, 1025
- . 2008b, *ApJ*, 679, 118
- Simpson, C. 2005, *MNRAS*, 360, 565
- Simpson, C., & Rawlings, S. 2000, *MNRAS*, 317, 1023
- Simpson, C., Rawlings, S., & Lacy, M. 1999, *MNRAS*, 306, 828
- Smith, E. P., Heckman, T. M., Bothun, G. D., Romanishin, W., & Balick, B. 1986, *ApJ*, 306, 64
- Soria, R., Fabbiano, G., Graham, A. W., Baldi, A., Elvis, M., Jerjen, H., Pellegrini, S., & Siemiginowska, A. 2006a, *ApJ*, 640, 126
- Soria, R., Graham, A. W., Fabbiano, G., Baldi, A., Elvis, M., Jerjen, H., Pellegrini, S., & Siemiginowska, A. 2006b, *ApJ*, 640, 143
- Steffen, A. T., Barger, A. J., Cowie, L. L., Mushotzky, R. F., & Yang, Y. 2003, *ApJL*, 596, L23
- Sulkanen, M. E., & Bregman, J. N. 2001, *ApJL*, 548, L131
- Tajer, M., et al. 2007, *A&A*, 467, 73
- Telfer, R. C., Zheng, W., Kriss, G. A., & Davidsen, A. F. 2002, *ApJ*, 565, 773
- Tran, H. D. 2003, *ApJ*, 583, 632
- Treister, E., Krolik, J. H., & Dullemond, C. 2008, *ApJ*, 679, 140
- Tremaine, S., et al. 2002, *ApJ*, 574, 740
- Ueda, Y., Akiyama, M., Ohta, K., & Miyaji, T. 2003, *ApJ*, 598, 886
- van Dokkum, P. G., et al. 2004, *ApJ*, 611, 703
- Vanden Berk, D. E., et al. 2001, *AJ*, 122, 549
- . 2006, *AJ*, 131, 84
- Vestergaard, M., & Peterson, B. M. 2006, *ApJ*, 641, 689
- Vignali, C., Brandt, W. N., & Schneider, D. P. 2003, *AJ*, 125, 433
- Volonteri, M., Salvaterra, R., & Haardt, F. 2006, *MNRAS*, 373, 121
- Weinzirl, T., Jogee, S., Khochfar, S., Burkert, A., & Kormendy, J. 2009, *ApJ*, 696, 411
- Weymann, R. J., Carswell, R. F., & Smith, M. G. 1981, *ARA&A*, 19, 41
- Willott, C. J., Rawlings, S., Blundell, K. M., & Lacy, M. 2000, *MNRAS*, 316, 449
- Younger, J. D., Hopkins, P. F., Cox, T. J., & Hernquist, L. 2008, *ApJ*, 686, 815
- Yu, Q., & Lu, Y. 2008, *ApJ*, 689, 732
- Yu, Q., Lu, Y., & Kauffmann, G. 2005, *ApJ*, 634, 901
- Yuan, F., & Narayan, R. 2004, *ApJ*, 612, 724
- Zakamska, N. L., Strauss, M. A., Heckman, T. M., Ivezić, Ž., & Krolik, J. H. 2004, *AJ*, 128, 1002
- Zakamska, N. L., et al. 2006, *AJ*, 132, 1496